Roles of climatic and anthropogenic factors in shaping Holocene vegetation and fire regimes in Great Dismal Swamp, eastern USA

D.A. Willard [a, *], M.C. Jones [a], J. Alder [b], D. Fastovich [c, d], K. Hoefke [a], R.K. Poirier [a], F.C. Wurster [e]

[a] U.S. Geological Survey, Florence Bascom Geoscience Center, MS 926A, Reston, VA, USA
[b] U.S. Geological Survey, Geology, Minerals, Energy, And Geophysics Science Center, Corvallis, OR, USA
[c] Department of Geography, University of Wisconsin, 550 N. Park St., Madison, WI, USA
[d] Department of Earth and Environmental Sciences, Syracuse University, 204 Heroy Geology Laboratory, Syracuse, NY, USA
[e] Great Dismal Swamp National Wildlife Refuge, 3100 Desert Road, Suffolk, VA, USA

ARTICLE INFO

ABSTRACT

The Great Dismal Swamp wetland, spanning >400 km² along the Virginia and North Carolina border, was shaped by a complex combination of geomorphic, climatic, and anthropogenic forcings during the last 14,000 years. Pollen, macrofossils, charcoal, and physical properties from sediment cores at seven sites provide a detailed record of the spatial heterogeneity of the wetland and the roles played by natural hydrologic variability, wildfire, and human modification of drainage in shaping vegetation and habitats. Cold-temperate forests occupied regional uplands from at least 13.5–10.3 cal ka BP. Marshes dominated by grasses and other herbaceous taxa began developing along low-elevation streams as early as 10.3 cal ka BP, resulting in accumulation of organic silts. Long-hydroperiod, peat accumulating marshes, with abundant floating aquatic plants, developed as early as 9.6 cal ka BP, as rapid rates of sea-level rise elevated the water table and facilitated wetland development and peat accumulation along stream courses. By the mid-Holocene (c. 7–6.5 cal ka BP), when local sea-level rise began slowing and reached about 12–15 m below present, shorter hydroperiod, peat-accumulating marshes dominated the landscape, with increased wildfire activity. Great Dismal Swamp vegetation shifted from marshes to peat-accumulating forested wetlands by c. 3.7 cal ka BP; these were dominated by varying combinations of *Nyssa* (tupelo), *Taxodium* (cypress), and *Chamaecyparis thyoides* (Atlantic white cedar). Wildfires were infrequent during this time, and the forested wetlands persisted, with minor compositional changes related to climate-driven fluctuations in stream flow, until colonial ditching and logging began in the swamp during the late 18th century. These activities decreased cypress and cedar populations, and, by the mid-20th century, expanded ditching resulted in even drier conditions and expansion of maple-gum (dominated by *Acer* and *Liquidambar*), and pine-pocosin (dominated by *Pinus*) forests. The distribution of these forests differs from that of the late Holocene and represents a fundamental shift in hydrology, peat structure, vegetation, and fire regime due to landscape alterations of the last few centuries.

1. Introduction

Wetlands provide many important ecosystem services, including provision of habitats for fish and wildlife, filtering of contaminants, and flood protection. Peatlands (wetlands accumulating partially decayed organic matter with >70% organic matter content) provide an additionally important service by sequestering and storing carbon over long timescales. Although wetlands occupied about 11% (nearly 900,000 km²) of the conterminous United States in the 17th century, their extent was more than halved by the late 20th century, when approximately 400,000 km² remained (Dahl and Allord, 1996). On a global scale, the composition and distribution of forested wetlands (swamps) have been affected by expansion of agriculture and urban areas, water management, and changing climate (King and Keim, 2019). Forested wetlands in woutheastern North America were reduced by 11% between 1940

* Corresponding author. U.S. Geological Survey, 12201 Sunrise Valley Dr., MS 926A, Reston, VA, 20192, USA.
E-mail address: dwillard@usgs.gov (D.A. Willard).

and 1980 CE (Abernethy and Turner, 1987), with resulting detrimental impacts on habitats, water quality, and accumulation of sediments and carbon (Hupp, 2000; Sharitz and Mitsch, 1993; Spieran and Wurster, 2020). The loss of such important ecosystem services has prompted management efforts to "restore" wetlands and re-establish either the original plant communities or those providing similar functions.

An important question in restoration ecology lies in the choice of targets for restored systems, and recent work has started to include paleoecological evidence that establishes baselines for climatic and hydrologic variability prior to significant human disturbance (Barak et al., 2016; Jackson and Hobbs, 2009; Manzano et al., 2020; Willard and Cronin, 2007). Integration of long-term paleoecological records with monitoring and instrumental studies can provide a better understanding of how wetland systems function over multiple time scales in response to natural stressors, such as fluctuations in temperature, precipitation, and sea level, as well as human-induced changes.

The Great Dismal Swamp (GDS), located on the outer Atlantic Coastal Plain of North America in southeastern Virginia and northeastern North Carolina (Fig. 1), is uniquely influenced by atmospheric processes, rising sea level, and changes in land management practices. This study uses evidence from multiple study sites in GDS National Wildlife Refuge (NWR) to examine how a combination of environmental stressors, including changing temperature, precipitation, sea level, and human modification of the landscape, have influenced GDS vegetation and fire regimes during the last c.13,500 years. Specifically, data on pollen, charcoal, plant macrofossils, and peat physical properties are used to reconstruct past vegetation, fire, and climate regimes, document patterns of wetland development during the Holocene, and evaluate how anthropogenic changes of the last few centuries have altered the structure and composition of the GDS forested wetland. In addition, we examine the potential to reconstruct the composition of regional to extralocal vegetation in adjacent forests from wetland sediments to expand the existing suite of climate and vegetation reconstructions based on estuarine and lacustrine sites in the eastern United States.

GDS lies in a climatic transition zone defined by the polar jet stream, which fluctuates between meridional and zonal flow patterns, influencing regional temperature, precipitation, and storm frequency on multidecadal to millennial time scales (Vega et al., 1998, 1999). The position of the polar jet is, in turn, related to the North Atlantic Oscillation (NAO), with meridional and zonal flow associated with negative and positive modes of the NAO, respectively (Hurrell, 1995). These fluctuations have been tied to millennial-scale shifts in winter temperatures, precipitation, regional forest composition, flood frequency, and tropical cyclone
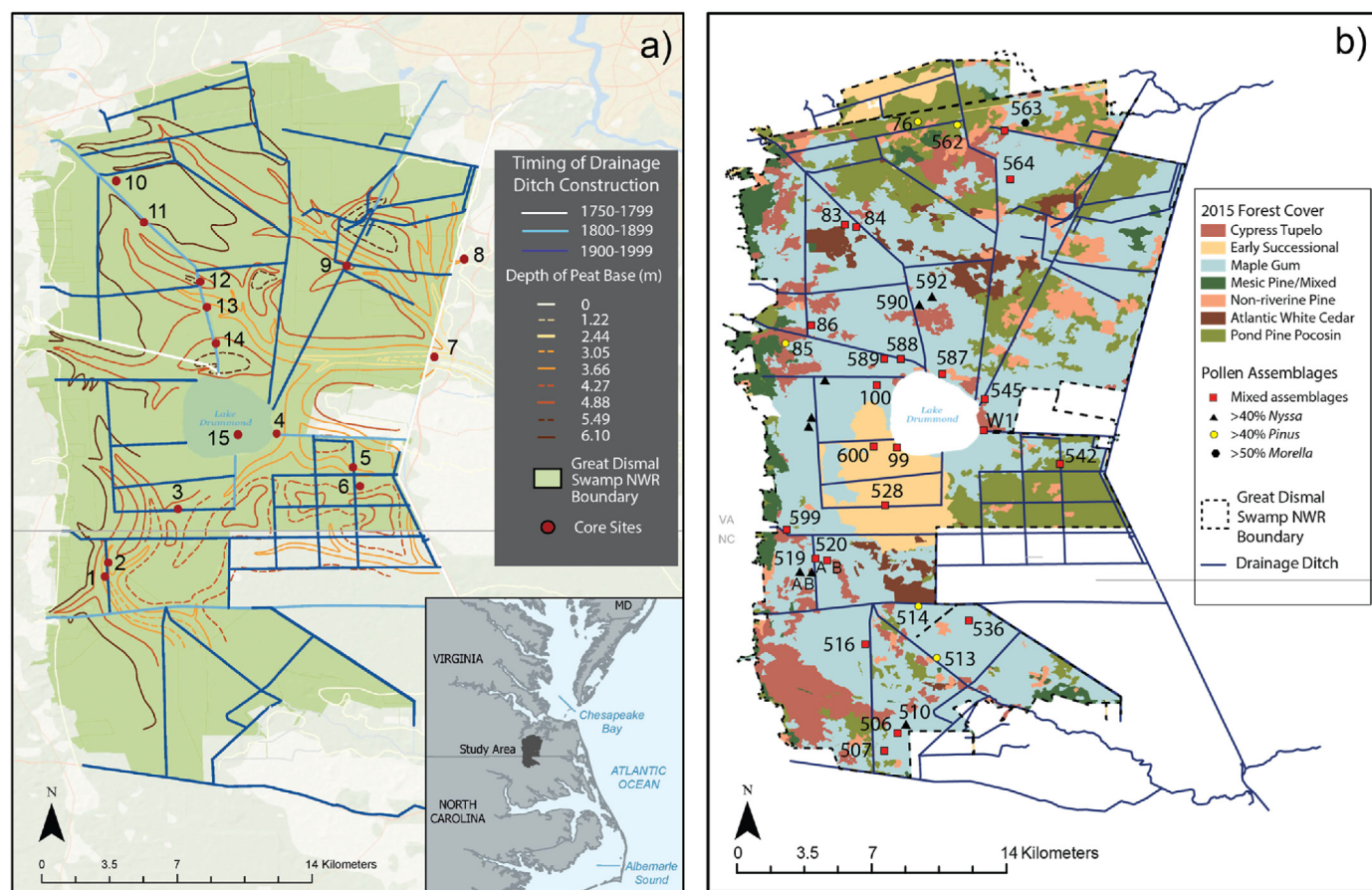

Fig. 1. Location of Great Dismal Swamp National Wildlife Refuge (GDS), canals, forest cover, and pollen sample sites. Inset map in panel a shows location of the study area in the mid-Atlantic region of the United States. a) GDS ditches and canals, topography of the peat base, and timing of drainage ditch construction. Coring locations are indicated by red dots, and numbers indicate core identifications in Table 1. Contour intervals are provided in meters. Base map from Oaks and Whitehead (1979). Timing of ditch construction from Trout (2004). Sites 7, 8, 10, and 12−15 represent locations sampled by previous investigators (Cocke et al., 1934; Lewis and Cocke, 1929; Whitehead, 1972). b) Forest cover of GDS (after Spieran and Wurster, 2020) and location of 36 surface samples analyzed for pollen. Locality information for surface sample sites is provided in Supplementary Table 1. Forest types were interpreted from 2015 imagery (Spieran and Wurster, 2020), and the area with early successional vegetation south and west of Lake Drummond was severely burned in 2008 and 2011. Types of modern pollen assemblage are indicated by shapes as outlined in legend.

generation that have been recorded in paleoclimate records from Chesapeake Bay and speleothems in West Virginia (Hardt et al., 2010; Saenger et al., 2006; Toomey et al., 2019; Willard et al., 2005).

The entire Atlantic Coastal Plain also has been inundated periodically by sea-level highstands since at least the mid-Pliocene, and the base of the Suffolk Scarp, a Marine Isotope Stage 5 (MIS 5) paleoshoreline, is the western boundary for GDS (Parham et al., 2013). Additional sediments were deposited on the Pamlico Terrace, east of the Suffolk Scarp after MIS 5, providing the geologic framework that underpins the modern GDS. Rising sea level since the Last Glacial Maximum (LGM) influenced the modern topography and hydrology of the region. .

Human modification of the landscape has also had significant impacts on GDS, which has been subjected to extensive ditching, logging, and other modifications since a company founded by George Washington and others began constructing ditches between 1763 and 1768 CE (Hansen, 2010). These modifications reduced the GDS area from >3900 km^2 in pre-Colonial time (Shaler, 1890) to its modern extent of approximately 500 km^2 (Spieran and Wurster, 2020), which includes both the Great Dismal Swamp National Wildlife Refuge (GDS NWR) and the Dismal Swamp State Park, North Carolina. Scientists and resource managers in both entities cooperate to protect the GDS ecosystem to provide habitat for wildlife, restore historic forest communities, reduce wildfire risk, and provide recreational services (Spieran and Wurster, 2020). To develop sustainable habitat management plans, managers and scientists are comparing recent data on the ecosystem with longer-term paleoecological data. This study provides insights into pre-drainage conditions as baselines to evaluate impacts of Holocene climate variability and human modifications of the landscape on wetland plant communities and fire regimes.

1.1. Geologic setting of Great Dismal Swamp

The Great Dismal Swamp is bordered on the west by the Suffolk Scarp, with an eastward decrease in elevation of about 0.3 m per 1.6 km to its eastern boundary at the Deep Creek Swale (Lichtler and Walker, 1974). Thick, impermeable, marine clays of the Pliocene Yorktown Formation underlie the area, providing a confining bed that is within 5−8 m of the surface (Oaks and Coch, 1963; Spieran and Wurster, 2020; U.S. Fish and Wildlife Service, 2006). The Late Pleistocene Tabb Formation overlies the Yorktown Formation, with its basal marine/estuarine Sedgefield Member

overlain by lagoonal clays/silts of the Lynnhaven Member, which is in turn overlain by marsh/tidal flat silty clays of the Poquoson Member (Oaks and Coch, 1963; Peebles et al., 1984; Mixon et al., 1989). During glacial-age low stands of sea level, a dendritic drainage pattern was incised into the top of the Poquoson Member (Fig. 1a), and sediment accumulation began in depressions along stream courses during the last deglaciation, shifting to peat accumulation across most of the GDS landscape by the mid-Holocene (Whitehead, 1972; Oaks and Whitehead, 1979).

1.2. Modern climate and vegetation of Great Dismal Swamp

Climate in the region is characterized by hot, humid summers and cool, low-humidity winters, with the mean annual temperature averaging 15.4 °C (based on data 1981−2010 CE data from the National Oceanic and Atmospheric Administration station at Suffolk, Lake Kilby, (station number USC00448192) (data accessed on 10 January 2022 from https://www.ncdc.noaa.gov/cdo-web/datatools/normals). Average minimum temperatures during this period were 0.6 °C, with maximum temperatures averaging 29.8 °C. Annual precipitation averaged 1257 mm, with most falling during the summer and early fall. Most fires in GDS presently result from lightning strikes, and they are most frequent during the summer, when more intense thunderstorms occur (Spieran and Wurster, 2020).

Great Dismal Swamp vegetation currently is dominated by forested wetlands with a limited occurrence of herbaceous-dominated marshes. The dominant forest type is referred to as a red maple-gum (*Acer rubrum/Nyssa sylvatica*) forest, which covers slightly more than 60% of the GDS landscape (Ludwig et al., 2021; Sleeter et al., 2017) (Fig. 1b). Maple-gum swamps occur on relatively well-drained peats, and few other tree species are present (Levy, 1991). Pine-dominated forests (including pond pine pocosin and non-riverine pine hardwood forests [Fig. 1b]) are dominated by pond pine (*Pinus serotina*), cover more than 15% of GDS NWR, and range from mature pine forests over shallow peats to stunted pine stands in seasonally flooded areas (Sleeter et al., 2017). Cypress-tupelo (*Taxodium distichum/Nyssa biflora*) forests occur in poorly drained, low-elevation areas that are subject to prolonged seasonal flooding; these forests have relatively low diversity and currently cover only about 12% of the Refuge (Shaler, 1890; Sleeter et al., 2017; Spieran and Wurster, 2020). The least common forest type, covering approximately 3% of GDS, is the Atlantic white cedar

Table 1
Location of coring sites in Great Dismal Swamp National Wildlife Refuge with map identifiers keyed to Fig. 1. Coring devices are noted, along with the total core length. Sites marked with asterisks represent those published by Cocke et al. (1934) (Sites 10, 12, 14), Lewis and Cocke (1929) (Site 7), and Whitehead (1972) (Sites 8, 13, 15). Locations for those sites were estimated based on maps and site descriptions in those publications.

Map ID	Core ID	Latitude (°N)	Longitude (°W)	Vegetation type	Core type	Core length (cm)
1	GDS-519B-3-21-2017	36.5292	76.5256	Cypress-tupelo swamp	Russian peat corer	350
2	GDS-520-3-21-2017	36.5359	76.5241	Maple-gum swamp	Russian peat corer	296
3	GDS-528-3-20-2017	36.5608	76.4917	Burned zone; early successional	Russian peat corer	244
3	GDS528-F-11-18-2020	36.5608	76.4917	Burned zone; early successional	Freeze corer	38
4	GDS-W1-05-09-2018-2	36.5959	76.4457	Maple-gum swamp	Russian peat corer	250
5	GDS-543-05-07-2018	36.5714	76.4069	Pine pocosin	Russian peat corer	235
6	GDS-542-05-08-2018	36.5802	76.4101	Pine pocosin	Russian peat corer	144
7	Lewis and Cocke (1929) site*	36.6316	76.3723	Maple-gum swamp	Davis peat borer	275
8	Whitehead (1972) Site DS-77*	36.6835	76.3605	Maple-gum swamp	Davis peat borer	220
9	GDS-P&H-04-13-2021	36.6741	76.4131	Maple-gum swamp	Russian peat corer	100
10	Cocke et al., (1934) station 1*	36.6609	76.5225	Maple-gum swamp	Davis peat borer	60
11	GDS-83-3-22-2017	36.6942	76.5075	Maple-gum swamp	Russian peat corer	150
12	Cocke et al., (1934) station 2*	36.6666	76.4813	Maple-gum swamp	Davis peat borer	150
13	Whitehead (1972) Site DS-49*	36.6547	76.4782	Maple-gum swamp	Hiller sampler - upper meter; Livingstone corer -lower sediments	390
14	Cocke et al., (1934) station 3*	36.6379	76.4740	Maple-gum swamp	Davis peat borer	275
15	Whitehead (1972) Site LD-59	36.5939	76.4616	Lake Drummond	Livingstone corer	240

(*Chamaecyparis thyoides*) community. Atlantic white cedar swamps require stable water levels and are dependent on large-scale disturbances like wildfire for regeneration (Shaler, 1890; Sleeter et al., 2017; Spieran and Wurster, 2020). Marshes, dominated by herbaceous plants with few trees or shrubs, currently are widespread only in areas with recent tree mortality due to wildfires or prolonged inundation.

1.3. Human modification of Great Dismal Swamp

Although Native American settlements have been documented archeologically on the western border of GDS and date to Early Archaic time (10-8 cal ka BP) (Bottoms and Painter, 1979), the most intensive activity occurred during the Late Archaic period (4.5−3.1 cal ka BP), based on recovery of Perkiomen points, knives, and discovery of what is interpreted as a storage pit for nut crops (Blanton, 2002, 2003; Egghart, 2020; McCary, 1972). Archeological evidence indicates that settlements were maintained along the margins of GDS through Middle Woodland time, with abandonment occurring after 1.8 cal ka BP (Nash, 2020). Potential evidence for Middle Woodland settlement within GDS is provided by the recovery of *Zea* (maize) pollen from a core collected near Lake Drummond at ~2.1 cal ka BP (Whitehead, 1965). During the 17th and early 18th centuries, Native American settlements were established within GDS, followed by "maroon" populations of self-emancipated African Americans, who lived in the swamp from c. 1730 CE until the Civil War (Sayers, 2006). Although GDS proper no longer is home to any significant human populations, the swamp presently is surrounded by farmland and cities.

Early Colonial exploration of the area included the discovery of Lake Drummond in 1665 CE by the North Carolina governor William Drummond and subsequent surveying of the area by a party led by William Byrd II to establish the Virginia-North Carolina border in 1728 CE (Stewart, 1979). By the 1760s, Dismal Swamp remained the last undeveloped tract of land in the Tidewater region of Virginia, and the Dismal Swamp Land Company was formed with George Washington among the founding members. Starting in 1763 CE, the Company built ditches to improve drainage and provide transportation for lumber and shingles (Stewart, 1979). In the 18th and 19th centuries, several ditches, including Washington's Ditch, Jericho Ditch, Dismal Swamp Canal, Hamburg Ditch/Cross Canal, the Feeder Ditch, and Portsmouth Ditch were constructed (Fig. 1a), but most of the GDS ditches were dug during the 20th century to facilitate drainage and further access to timber (Trout, 2004). In 1974 CE, the Union Camp Corporation donated approximately 200 km^2 into conservation status, which resulted in establishment of the Great Dismal Swamp NWR. Although the area currently is held in conservation status, the legacy of past logging remains in the network of more than 300 km of ditches and associated logging roads on GDS NWR and Dismal Swamp State Park in North Carolina.

1.4. Fire history of Great Dismal Swamp

Historically, fires have been documented as far back as 1806 CE, when large fires burned areas from which timber had been harvested (Simpson, 1990; Stewart, 1979). Prior to colonial times, Native Americans in the Virginia and North Carolina Coastal Plain are known to have used fire for hunting and agriculture (Hammett, 1992), but these are thought to have been low intensity brush fires (Fowler and Konopik, 2007). After 1900 CE, fire frequency increased along with railroad and timbering activity; these activities typically occurred during dry periods, and a particularly severe fire ("The Great Conflagration") burned from 1923 to 1926 CE, affecting >400 km^2 of GDS and air quality in the nearby Hampton Roads area (Simpson, 1990).

Fire suppression activities, initiated in the mid-20th century, have reduced fire frequency and severity, and lightning strikes now are the primary ignition source (USFWS, 2006). However, the South One fire in 2008 CE was started by a mechanical spark and burned nearly 20 km^2 over more than 120 days (Sleeter et al., 2017; Spieran and Wurster, 2020). The same area burned again in 2011 CE, during the Lateral West fire, which was started by lightning and burned more than 25 km^2 in more than 100 days (Sleeter et al., 2017). Collectively, the 2008 and 2011 fires resulted in a conversion of forested wetlands to marshes described as early successional vegetation in Fig. 1b.

2. Materials and methods

2.1. Study area and core sampling

Locations for sediment coring were identified in each of the four primary vegetation types near vegetation study sites of Ludwig (2018) and hydrologic monitoring sites established by GDS staff (Fig. 1a, Table 1). At each site, sediments were probed to identify locations of maximum sediment thickness; root and leaf mats were cut and removed using hand tools before collection of cores with a Russian corer. For sites with poor recovery in the uppermost 50 cm drive, a freeze corer was used to capture the uppermost sediments. Pollen also was isolated from 36 surface samples from vegetational monitoring sites of Ludwig (2018) (Fig. 1b). Sediment cores were imaged using a Geotek Multi-Sensor Core Logger at the U.S. Geological Survey Florence Bascom Geoscience Center in Reston, Virginia before description and sampling. Cores were sampled at 1 cm increments for analysis of bulk density, loss-on-ignition (LOI), pollen, plant macrofossils, and charcoal. Bulk density and LOI were measured on each sample. Pollen, plant macrofossil, and charcoal analyses were performed more coarsely, with sampling intervals ranging from 2 to 10 cm.

2.2. Core physical properties

Cores collected with a Russian corer were subsampled into 1 cm increments, sampling 1 cm^3 of sediment for LOI and bulk density using standard procedures (Dean, 1974). Each 1 cm^3 sample was weighed wet in a crucible and dried at 50 °C for at least 24 h. Dry samples were re-weighed and burned in a furnace at 550 °C for 4 h. The remaining ash was then reweighed. Bulk density was calculated by dividing the original volume by the dry weight. LOI was calculated by subtracting the burned weight from the dry weight and dividing by the dry weight.

Freeze cores were subsampled at 2 cm increments in the field, and volume was measured on the whole frozen sample using calipers. Whole core samples were weighed in the laboratory in Reston, Virginia and subsampled for LOI following procedures for Russian core samples above.

2.3. Pollen analysis

Samples for pollen analysis were dried and weighed before addition of one *Lycopodium* marker tablet for calculation of absolute pollen concentrations (Stockmarr, 1971). Pollen analysis used standard techniques (Traverse, 2007; Willard et al., 2011), including demineralization with HCl and HF, acetolysis, and sieving with 150 μm and 10 μm mesh to remove coarse residue and clays, respectively. Pollen residue was stained with Bismarck Brown and mounted in glycerin jelly. Residues are stored in ethanol and curated in the U.S. Geological Survey palynological working collections in Reston, Virginia. Pollen data, along with other ancillary data, are reposited in the Neotoma Paleoecology Database (https://

www.neotomadb.org/), and surface sample datasets also are reposited at the National Center for Environmental Information (https://www.ncei.noaa.gov).

Because raw data from pollen analyses conducted by Donald R. Whitehead (1972) are unavailable, the pollen residues from that study were obtained from Whitehead's collections, mounted on microscope slides in glycerin jelly, and counted. Those collections originally were curated by S.T. Jackson at the University of Arizona and now are housed in the palynological research collections of the Florence Bascom Geoscience Center in Reston, Virginia. Results of new counts from Whitehead's sites DS-49 and DS-77 are included with this study.

It is worth noting that morphological similarities between *Taxodium* and *Chamaecyparis* pollen and infrequent preservation of the few distinctive characters of the genera (such as presence/absence of a papilla) preclude consistent identification beyond the family level. *Pinus* species are virtually impossible to distinguish based on pollen size (Whitehead, 1964), although some taxa (e.g., *P. strobus*) have distinctive morphologic characters that facilitate their identification. *Pinus banksiana* and *P. resinosa* produce small pollen grains and are restricted geographically to New England and farther north (Thompson et al., 1999a), and we identified pine grains smaller than 50 μm as *P. banksiana*-type. Pollen from *Acer* species in the northeastern United States are characterized by three types of ornamentation (striate, rugulose, and microreticulate) (Philbrick and Bogle, 1981). *Acer* pollen identified from GDS samples is striate, typically have gaping colpi, and likely were produced by *A. rubrum* (see descriptions in Philbrick and Bogle, 1981).

2.4. Plant macrofossil and charcoal analysis

Plant macrofossil analysis is based on the method described in Mauquoy et al. (2010). Briefly, 1 cm^3 of peat or sediment was washed through a 250 μm sieve. Material remaining on the sieve was washed into a gridded Petri dish with deionized water. Relative abundances of the main peat composition (ligneous, herbaceous, bryophytic, and unidentifiable detritus) were surveyed using a stereomicroscope. Discrete seeds, needles, and leaves were identified to genus or species level, and tallied. Wood fragments were not taxonomically identified, but the presence/absence of wood with a reddish hue was noted, indicating the likely presence of trees in the Cupressaceae family.

Charcoal was counted separately from the macrofossil counts by using de-ionized water to wash 1 cm^3 of sample through nested sieves of 125 μm, 250 μm, and 500 μm mesh sizes. Sample material from each sieve was washed into a gridded Petri dish and tallied. For this study, results of the >125 μm fraction are presented as charcoal accumulation rates (CHAR) by multiplying the total charcoal counts by the sedimentation rate calculated from the age model results.

2.5. Geochronology

Age-depth models for GDS cores are based on a combination of radiocarbon dates and pollen biostratigraphy. Although ^{210}Pb analyses were conducted on the cores, the results from most cores were inconsistent with pollen biostratigraphy and radiocarbon dates. Previous research indicated that these radioisotopes are highly mobile in GDS peats, due to water movement through the porous upper layers of peat (Drexler et al., 2017), and concentrations in these records varied widely downcore, rather than following a standard decay curve. In addition, in some cases, ^{210}Pb reached background values below the *Ambrosia* pollen peak, dated at 1800 CE (see discussion below), indicating migration of the radioisotope through the water column. Therefore, ^{210}Pb age

models were not incorporated into age models for GDS cores. When possible, radiocarbon dates were obtained on aerial plant macrofossils or charcoal; where no identifiable material was available, dates were obtained on the fine fraction (<63 μm) of the bulk sediment and pollen residue. Preparation of pollen residue for radiocarbon dating consisted only of demineralization with HCl and HF and sieving with 10 μm and 150 μm mesh to avoid contamination with organic solvents (Brown et al., 1989). Radiocarbon dates were calibrated using the IntCal20 calibration curve (Stuiver et al., 2022) and are presented in Supplementary Table 2.

Pollen biostratigraphy was based on changes in abundance of taxa influenced primarily by land cover changes, including *Ambrosia* and *Acer*. *Ambrosia* is an early successional plant that rapidly occupies cleared land (Bazzaz, 1974; Keever, 1983), and increased abundance of its pollen has been used as a stratigraphic marker of deforestation in much of eastern North America (Brush, 1984; McAndrews, 1988). Production of *Ambrosia* pollen also is enhanced by increased CO_2 concentrations (Ziska and Caulfield, 2000), and increased CO_2 concentrations since the start of the Industrial Revolution in the mid-19th century may have contributed to higher proportions of *Ambrosia* in the pollen rain. Although *Ambrosia* is rare within GDS, clearance of upland forests surrounding the swamp is well documented since the 19th century. Colonists established plantations along the nearby Nansemond River in the early 17th century (Bottoms, 1983), and aggressive land clearance for timber started in earnest in the late 18th century, when the Dismal Swamp Land Company and the Adventurers for Draining the Great Dismal Swamp were formed (Hansen, 2010). Although the most significant increases in *Ambrosia* pollen abundance would have been recorded in upland deposits, its abundance also increased in assemblages from GDS. Based on the land-use history indicating most significant clearance in the late 18th century and comparison with baseline abundances of *Ambrosia* in late Holocene GDS pollen records, we assigned the date of 1800 CE ± 20 (0.15±0.02 cal ka BP) to the depth where *Ambrosia* pollen exceeded 2% abundance. In the mid-20th century, a larger network of canals was dug throughout the swamp to facilitate logging, and a doubling in abundance of *Acer* pollen was assigned a date of 1960 CE ± 10 (−0.01±0.01 cal ka BP) at all sites affected by ditching and logging in the mid-20th century.

Bacon software for Bayesian modeling in R (Blaauw and Christen, 2011) was used to construct age-depth models that incorporate uncertainty estimates for dates and depths. Input included radiocarbon dates and pollen-based estimates for onset of colonial land clearance in the area and mid-20th century ditching as outlined above.

2.6. Statistical analyses and fossil pollen − paleoclimate reconstructions

Statistical analyses of pollen data are based on all taxa comprising ≥1% of assemblages in one or more samples. *Ambrosia* (ragweed) pollen was excluded from percentage calculations because its abundance was influenced more by human modification of the landscape than by climatic variability (Willard et al., 2011). Detrended correspondence analysis and cluster analyses were conducted using PAST (Paleontological Statistics) software (Hammer et al., 2001), and pollen zonations were guided by cluster analysis using the incremental sum-of-squares method (CONISS) (Grimm, 1987).

We reconstructed mean annual temperature (MAT), maximum temperature warmest month (MTWA) minimum temperature coolest month (MTCO), and mean annual precipitation (MAP) from the late-Pleistocene through the Holocene using the modern analog technique (Overpeck et al., 1985) trained on the North America

Modern Pollen Database (NAMPD, Whitmore et al., 2005). Samples collected before 1960 CE were excluded from the NAMPD (Whitmore et al., 2005), and the wetland surface samples added in this study were collected from 1995 to 2017 CE. The modern analog technique is a nearest-neighbor approach to reconstruct past climates from microfossil assemblages, where fossil-pollen counts in a sedimentary archive are matched to the most similar pollen abundances in a modern training dataset (i.e. modern analogs, Chevalier et al., 2020; Overpeck et al., 1985). Once one or more modern analogs are identified in the modern pollen training dataset, the contemporary climate parameters at the modern pollen analog sites are averaged and assumed to represent past climate conditions (Jackson and Williams, 2004). This process is then repeated for all fossil-pollen abundances in a sedimentary archive, thereby reconstructing past climate change through time. Analog quality can greatly influence confidence in modern analog technique-based climate reconstructions which we assess using Monte Carlo resampling (Sawada et al., 2004). Monte Carlo resampling assesses the likelihood that two randomly sampled modern pollen spectra are analogs by comparing two randomly sampled sites from the NAMPD and retaining their dissimilarities, from which we select a *p*-value of 5% as a threshold that discriminates analog and no-analog assemblages (Sawada et al., 2004). The modern analog technique has been used widely to reconstruct past environments successfully and has been instrumental in constraining climate change since the end of the LGM and through the Holocene, globally and in eastern North America (e.g. Bartlein et al., 2011; Fastovich et al., 2020; Marsicek et al., 2018). All reconstructions were performed using the *rioja* R-package (Juggins, 2015) in the R programming language (R Core Team, 2021) using the 64 taxa list in Williams and Shuman (2008) with geographic splits for *Picea* and *Pinus*. Monte Carlo resampling of modern pollen spectra was performed using the *analog* R-package (Simpson, 2007).

Several factors can complicate fossil-pollen climate reconstructions, which we address in our methodology. First, fossil pollen is commonly identifiable to the genus or family level, with only select pollen morphotypes identifiable to the species level. This is problematic as several genera in the NAMPD have contrasting climate preferences at the species level. For instance, *Pinus* occupies wide ranges in North America and includes species that prefer a range of climatic conditions that can produce confounding reconstructions (Thompson et al., 1999a, 1999b, 2000; Williams et al., 2006). To address this issue, we geographically split *Pinus* into northeastern and southeastern populations, each with distinct climatic preferences (Thompson et al., 1999a; Williams et al., 2006; Williams and Shuman, 2008). Under the recommendations of Williams and Shuman (2008), we minimize the effect of within-genera contrasting climate preferences by reducing the NAMPD to sites that only contain eastern species of *Picea* (e.g. *P. glauca, P. mariana,* and *P. rubens*). We perform both procedures using the shapefiles provided in the supplementary information of Williams and Shuman (2008). Due to geographic uncertainty in the ranges of eastern and western *Picea* species and northeastern and southeastern *Pinus* species, several sites in the NAMPD were identified as residing in the eastern and western ranges of *Picea* and the northeastern and southeastern ranges of *Pinus*. These sites were removed because of this ambiguity. We perform this *Pinus* splitting procedure in the fossil-pollen abundances based on grain size analyses because northeastern species of *Pinus* tend to have larger pollen grains and southeastern species of *Pinus* have smaller grains (Jackson et al., 2000; Watts, 1970; Whitehead, 1964). We define the local extinction of northeastern species of *Pinus* at 220.5 cm (5.4 cal ka BP) in DS49, 336 cm (13.0 cal ka BP) in GDS519, 280 cm (12.9 cal ka BP) in GDS520, 200.5 cm (5.3 cal ka BP) in GDS528, 102.5 cm

(10.5 cal ka BP) in GDS542, and 249 cm (13.4 cal ka BP) in GDSW1. Second, we use the average climate conditions of the seven nearest analogs in the NAMPD (Marsicek et al., 2018; Williams and Shuman, 2008) which minimizes the influences of any individual analog. Lastly, we incorporate new modern pollen abundances for 119 locations in the Roanoke River Basin and 30 locations in the GDS region, which better capture the local, forested wetland conditions likely present in the fossil-pollen abundances. Mean annual temperature, mean annual precipitation, and mean minimum temperature at these locations were bilinearly interpolated from the Climatic Research Unit gridded Time Series (Harris et al., 2020). As in Whitmore et al. (2005), we use the long-term mean from 1961 to 1990 CE for these climate variables but do not perform lapse rate adjustments.

After expanding the NAMPD with our new modern pollen samples and geographically splitting subpopulations of *Pinus* (southeastern/northeastern *Pinus* species), we trained our modern analog technique models and cross-validated using *h*-block cross-validation. *h*-block cross-validation assesses modern analog technique model performance by dividing the NAMPD into a test set and training set, where the test set is *h* kilometers away from the training set, thereby minimizing the effects of spatial autocorrelation and better assessing model performance (Telford and Birks, 2009). We follow recommendations from Trachsel and Telford (2016) to estimate *h* by calculating the empirical variogram of the detrended modern analog technique model training set residuals using the *gstat* R-package (Pebesma, 2004). We then fit variogram models to these empirical variograms to determine the distance at which spatial autocorrelation was negligible (e.g. fit variogram range) and used these values as estimates of *h*. Ranges for mean annual temperature, mean minimum temperature, and mean annual precipitation varied between 600 and 800 km. Using these values in *h*-block cross-validation demonstrated that mean annual temperature reconstructions were quite skillful ($r^2 = \sim 0.95$) while mean minimum temperature ($r^2 = \sim 0.4$) and mean annual precipitation ($r^2 = \sim 0.4$) modern analog technique models were less skillful at reconstructing values in the test dataset. Despite greater error in the mean minimum temperature and mean annual precipitation reconstructions, the history of aridity during the Holocene in eastern North America (Marsicek et al., 2013; Newby et al., 2014; Shuman et al., 2001) and the importance of minimum temperature and annual precipitation as biologically relevant climate variables suggests that these reconstructions are likely robust, albeit more uncertain than mean annual temperature.

2.7. Climate model data

We draw long-term modeled temperature and precipitation time series from the TraCE-21 K (Liu et al., 2009) transient climate simulation for comparison with our reconstructed climate. TraCE-21 K is a low resolution ($\sim 3.75° \times 3.75°$) simulation driven by the major climate forcings from the LGM to present, including the time evolving changes in greenhouse gas concentrations, orbital configuration and insolation, the presence and collapse of large Northern Hemisphere ice sheets with the corresponding meltwater flux into the oceans. TraCE-21 K has been widely applied to paleoclimate research to aid in the interpretation of proxy records and understanding the climate system response throughout the last deglaciation and Holocene (Liu et al., 2021). We extract mean annual temperature (MAT), mean temperature of the warmest month (MTWA), mean temperature of the coolest month (MTCO), and mean annual total precipitation (MAP). Due to the low resolution of the model and GDS proximity to the coast, we create regional time series from the surrounding four land-based model grid cells using inverse distance weighted (IDW) interpolation.

Modeled time series are averaged from annual to centennial time scales and standardized to z-scores for comparison to the reconstructed climate variables. The model simulations likely do not capture the nuance of change in relative sea level on the local climate of GDS but provide a useful benchmark for the surrounding climate throughout the Holocene.

3. Results

3.1. Lithology and chronology

Sediment cores from each site recovered similar lithologic sequences, consisting of basal silty clays (LOI<5%) that overlie the Poquoson Member of the Tabb Formation (Oaks, 1965; Mixon et al., 1989; Whitehead, 1972; Oaks and Whitehead, 1979) which grade into an organic silty clay (LOI 5−40%), which is overlain by a peaty silt (LOI 40−70%), and then a well-consolidated peat (LOI>70%). The uppermost peat layers have a coarse, sub-angular, blocky texture (Word et al., 2022). Locally described as "coffee-grounds" peats (Spieran and Wurster, 2020), these peats consist of humified masses of peat that are <0.5 mm in size with large interstitial pore spaces and a high pore-water content when soils are saturated. These coffee-ground peats extend as far as 50 cm below the surface, indicating the depth to which the peat can dry out due to a combination of seasonal water table fluctuations and dewatering from drainage ditches (Spieran and Wurster, 2020).

Peat thickness across GDS varies from a few centimeters to nearly 4 m, with thickest accumulations reported in topographic lows in the underlying silty clays of the Poquoson Member (Whitehead, 1972). Of the sites in this study, the thickest sediments occur at site GDS-519, where the 350-cm long core included 291 cm of peat (Table 2). This approaches the maximum reported peat thickness of 386 cm at a site on the north side of the Hamburg Ditch (Cross Canal) about 0.8 km east of the Sherrill Ditch (Oaks, 1965).

The oldest sediments recovered from GDS are silty clays that date to 13.5−13.3 cal ka BP at sites GDS-519, 520, 542, and W1 (Table 2). These sites are located at the lowest elevation associated with the paleodrainage system identified by Oaks (1965) and Oaks and Whitehead (1979) (Fig. 1a). At higher-elevation sites, basal dates on silty clays are progressively younger, ranging from 10.2 cal ka BP at a lower elevation site (GDS-528) to 6.7 cal ka BP at the highest elevation site (GDS-83). Likewise, the transition from silty clay to organic silt (LOI 5−40%) is earliest at the lowest elevation sites, ranging from 11.9 to 10.4 cal ka BP at sites GDS-519 and GDS-520 to as late as 2.8 cal ka BP at the highest elevation site GDS-83. The organic silt to silty peat (LOI 40−70%) transition ranged from 8.4 cal ka BP at GDS-520 to 5.8 cal ka BP at GDS-528, and the transition to a "true" peat (LOI>70%) ranges from 10 cal ka BP at GDS-519 to 2.6 cal ka BP at GDS-83 (Fig. 4). The depth of the transition from well-consolidated to "coffee-grounds" peat varies with the date and degree of ditching and site proximity to ditches.

3.2. Pollen assemblages from Great Dismal Swamp surface samples

Pollen assemblages from the four forested wetland types indicate that extralocal pollen (sensu Janssen, 1984), derived from plants growing in the nearby uplands, was well-represented in GDS surface samples. Extralocal pollen consists primarily of *Quercus* and

Table 2
Basal depth and ages from sediment cores collected from Great Dismal Swamp National Wildlife Refuge. Depths and ages of the clay to organic silt transition are provided, along with estimates of the topographic elevation of the basal peat, based on Fig. 1a. The silty clay to organic silt transition was identified by LOI >5%. The transition from organic silt to peaty silt corresponds to the depth where LOI values exceed 40%, and the transition to peat corresponds to the depth where LOI values exceed 70%. Asterisks (*) indicate sites published in Whitehead (1972), Cocke et al. (1934), and Lewis and Cocke (1929). Double asterisk at Whitehead (1972) Site LD-59, collected in Lake Drummond, notes the depth of transition from sand to peat. The cross (†) marks the site (GDS-542) with a depositional hiatus between 13.5 and 5.5 ka, which complicates identification of the timing of lithologic transitions.

Map ID	Core ID	Core length (cm)	Basal age of core (cal ka)	Depth of silty clay to organic silt transition (cm)	Age of silty clay to organic silt transition (cal ka)	Depth of organic-silt to silty peat transition (cm)	Age of organic-silt to silty peat transition (cal ka)	Depth of silty peat to peat transition (cm)	Age of silty peat to peat transition (cal ka)	Approximate elevation of peat base (m) (after Oaks and Whitehead, 1979)
1	GDS-519B-3-21-2017	350	13.5	311	11.9	−	−	291	10	3.05
2	GDS-520-3-21-17	296	13.4	257	10.4	240	7.1	224	7	3.66
3	GDS-528-3-20-2017	244	10.2	238	9.6	213	5.5	211	5.5	4.5
4	GDSW1-05-09-2018-2	250	13.3	220	10.4	201	7	164	7	4
5	GDS-543-05-07-2018	235	−	205	−	−	−	−	−	3.66
6	GDS-542-05-08-2018†	144	13.5	98	5.5	86	4.5	80	4.4	4
7	Lewis and Cocke (1929) site*	305	−	−	−	−	−	−	−	1.22
8	Whitehead (1972) DS-77*	220	−	170	−	−	−	140	−	3.66
9	GDS-P&H-04-13-2021	100	−	64	−	57	−	39	−	4.88
10	Cocke et al., (1934) station 1*	61	−	−	−	−	−	−	−	>6.1
11	GDS-83-2-33-2017	150	6.7	113	2.8	−	−	96	2.6	6.1
12	Cocke et al., (1934) station 2*	152	−	−	−	−	−	−	−	5.49
13	Whitehead (1972) Site DS-49*	390	>8.5	−	−	−	−	330	8.3	4
14	Cocke et al., (1934) station 3*	275	−	>244	−	−	−	−	−	5
15	Whitehead (1972) Site LD-59**	240	>4.7	~230**	~4.7	−	−	−	−	NA

Pinus pollen, with background values of up to 20% and 10%, respectively. Local differences in forested wetland type also are recorded by pollen assemblages. Although surface samples were collected in each of the four primary vegetation types, pollen assemblages fell into three primary groups: those dominated by *Pinus* pollen (>40% *Pinus*), those dominated by *Nyssa* pollen (>40% *Nyssa*), and those with mixed assemblages (Fig. 1b). *Pinus*-dominated assemblages were collected in and near pine-pocosin forests and disturbed areas. These assemblages typically have higher percentages of pollen of mesic taxa, including *Liquidambar, Carya, Acer, Morella*, and *Ilex*. Cluster analysis of surface pollen assemblages from GDS and forested wetlands along the Roanoke River in the Atlantic Coastal Plain (Fig. 2) indicates that the *Pinus*-dominated assemblages from GDS cluster with bottomland hardwood forests located on levees and transitional areas in the Roanoke River floodplain. Those from northernmost GDS, collected near the railroad and several canals, cluster with high-levee bottomland hardwood forests with median annual hydroperiods of <50 days per year, whereas those in western and southern GDS cluster with wet and mesic bottomland hardwood forests with median annual hydroperiods ranging from 40 to 175 days per year.

The *Nyssa*-dominated assemblages from GDS were collected in cypress-tupelo and maple-gum swamps with thick peat deposits, and they are generally located in the western part of GDS (Fig. 1b).
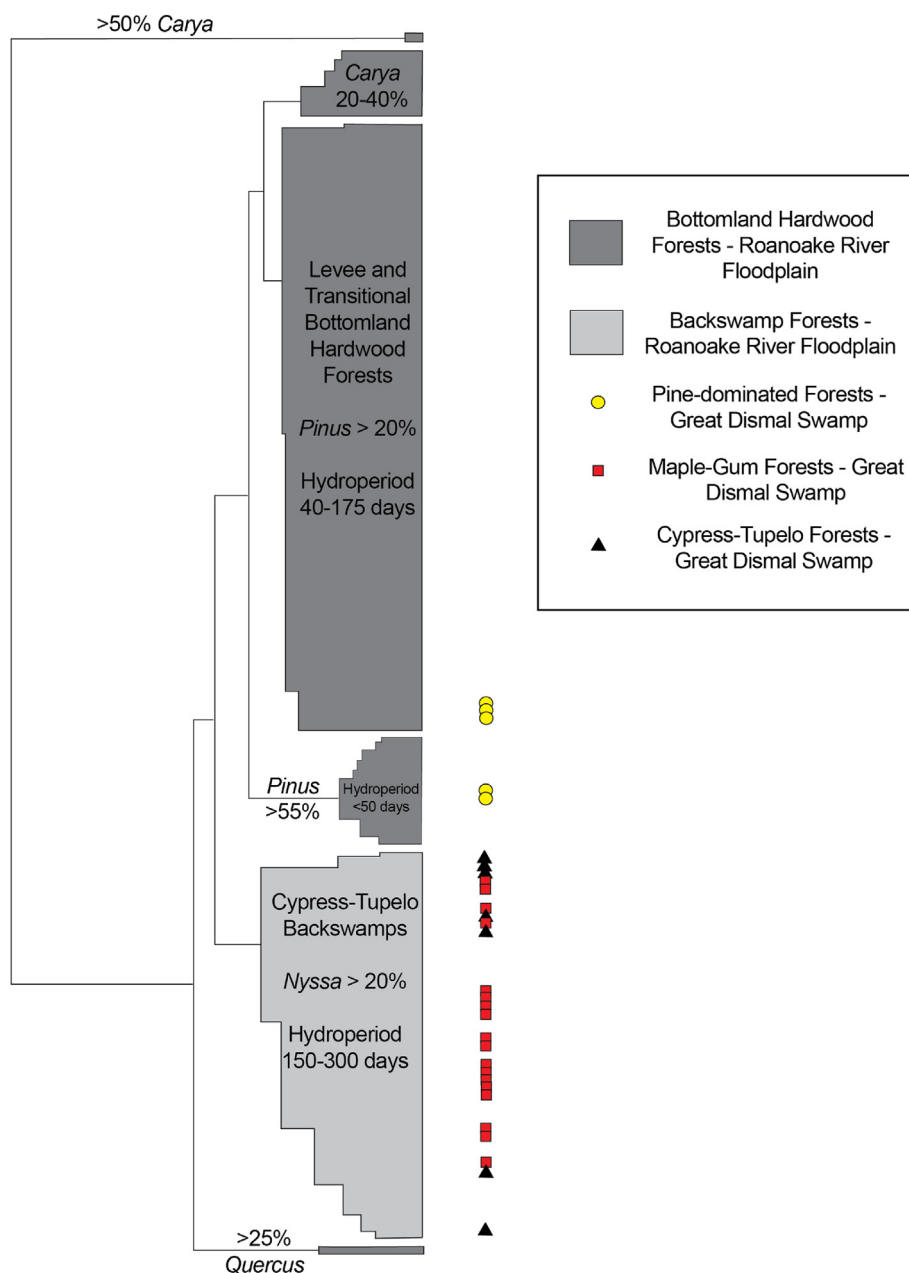

Fig. 2. Dendrogram from Q-mode cluster analysis of pollen data from surface samples collected in Great Dismal Swamp (indicated by circles, squares, and triangles) and the lower Roanoke River floodplain on the Coastal Plain of North Carolina. The cluster outlined by the light gray box represents Roanoke River floodplain samples collected in cypress-tupelo backswamps, characterized by long hydroperiods. Clusters outlined by darker gray boxes represent Roanoke River floodplain samples collected in bottomland hardwood forests on levees and transitional sites, with shorter hydroperiods. All of the GDS samples collected from maple-gum and cypress-tupelo forests cluster with long-hydroperiod sites from the Roanoke River floodplain, whereas pine-dominated sites cluster with short hydroperiod forests from Roanoke.

Mixed pollen assemblages include common *Nyssa*, Cupressaceae, *Pinus*, *Quercus*, *Acer* and/or *Liquidambar* pollen, and these were collected primarily in maple-gum swamps or, in some cases, on the drained side of ditches in cypress-tupelo swamps (Fig. 1b). The *Nyssa*-dominated and mixed pollen assemblages all cluster with cypress-tupelo backswamp forests from the Roanoke River floodplain, which have median annual hydroperiods ranging from 150 to 300 days per year.

3.3. Sediment cores − pollen assemblages and charcoal content

Of the six new sites examined in this study, four of the cores (GDS-519, GDS-520, GDS-W1, and GDS-542) recovered sediments from 13.3 to 13.5 cal ka BP, and cores from GDS-528 and GDS-83 recovered the last 10.2 and 6.7 cal ka BP, respectively (Table 2). Cores from sites GDS-519 and GDS-520 are the most densely sampled and are used to illustrate the general patterns of vegetational change through time in GDS (Fig. 3). Pollen zones in each

core were established based on visual inspection of data and results of stratigraphically constrained cluster analysis for each core. In addition, cluster analysis of every sample from each core facilitated identification of consistent pollen zonation across sites. Pollen diagrams for cores GDS-542, GDS-W1, GDS-83, GDS-528, DS-77, and DS-49 are presented in Supplemental Figs. 1−6.

3.3.1. Oak-pine zone (13.5−11.6 cal ka BP)

Basal silty clays deposited between 13.5 and 11.6 cal ka BP at sites GDS-519, -520, -W1, and -542 are characterized by low organic content (LOI <5%) and pollen assemblages with abundant *Pinus* and *Quercus* and common *Picea* (Fig. 3, Supplemental Figs. 1 and 2). *Abies* and *Pinus banksiana*-type pollen also are present. At site GDS-519, *Fagus* pollen is common from 13.5 to 12.9 cal ka BP (Fig. 3a); at the easternmost site, GDS-542, *Alnus* pollen comprises up to 80% of assemblages (Supplemental Fig. 1). Pollen concentrations are low (<200,000 grains g^{-1}), and charcoal is rare to absent.
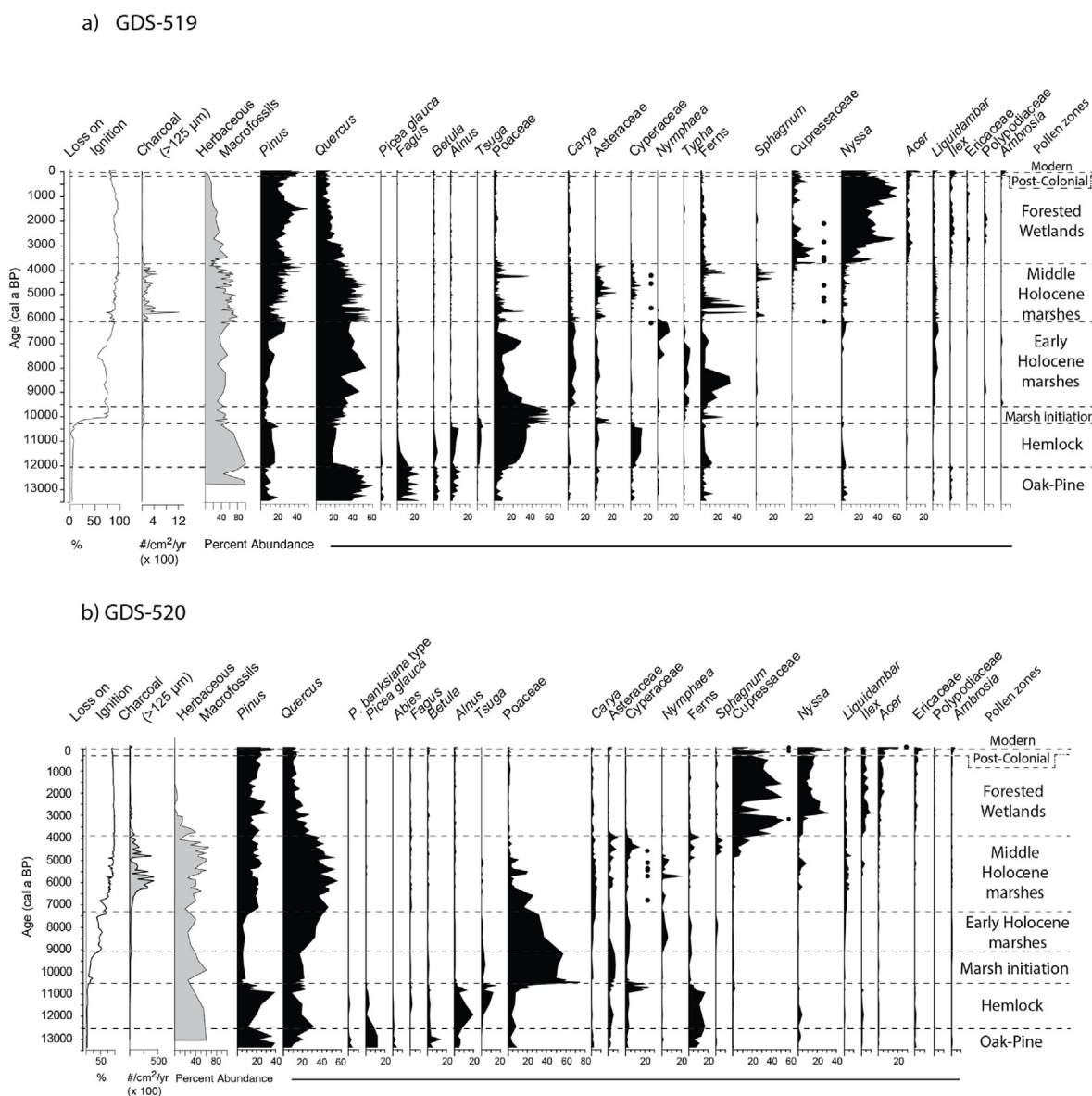
a) GDS-519

b) GDS-520

Fig. 3. Pollen abundance, charcoal, loss-on-ignition (LOI), and herbaceous macrofossil abundance vs. age in cores a) GDS-519B-3-17-2017 and b) GDS-520-3-17-2017. Pollen, LOI, and herbaceous macrofossil abundance are presented as percentages, and charcoal accumulation rates are presented as particles cm^{-2} yr^{-1}. Filled circles indicate presence of plant macrofossils. Boundaries for pollen zones are indicated by dashed lines.

3.3.2. Hemlock zone (11.6−10.3 cal ka BP)

Maximum abundances of *Tsuga* (up to 14%) occur in the Hemlock zone, and Poaceae pollen abundance approaches 40% in the upper part of the zone at GDS-519. Organic content is greater than in the Oak-Pine zone, with LOI of organic silts in this zone ranging from 5 to 10%; pollen concentrations are slightly higher than in the lower zones (up to 500,000 grains g^{-1}), and little charcoal was present.

3.3.3. Marsh initiation zone (10.3−9.6 cal ka BP)

Poaceae pollen strongly dominates assemblages in this zone, comprising 60−80% of assemblages (Fig. 3). The sediment is an organic silt that grades into a true peat at GDS-519 (Fig. 4). Pollen concentrations are higher in this zone, typically exceeding 500,000 grains g^{-1}; charcoal is present in this zone in low concentrations, with a small peak (up to 89 particles cm^{-2} yr^{-1}) visible at GDS-519 from 10.2 to 9.8 cal ka BP. This zone spans only 10−15 cm at sites GDS-519 and GDS-520 and was not observed at other sites (Figs. 3
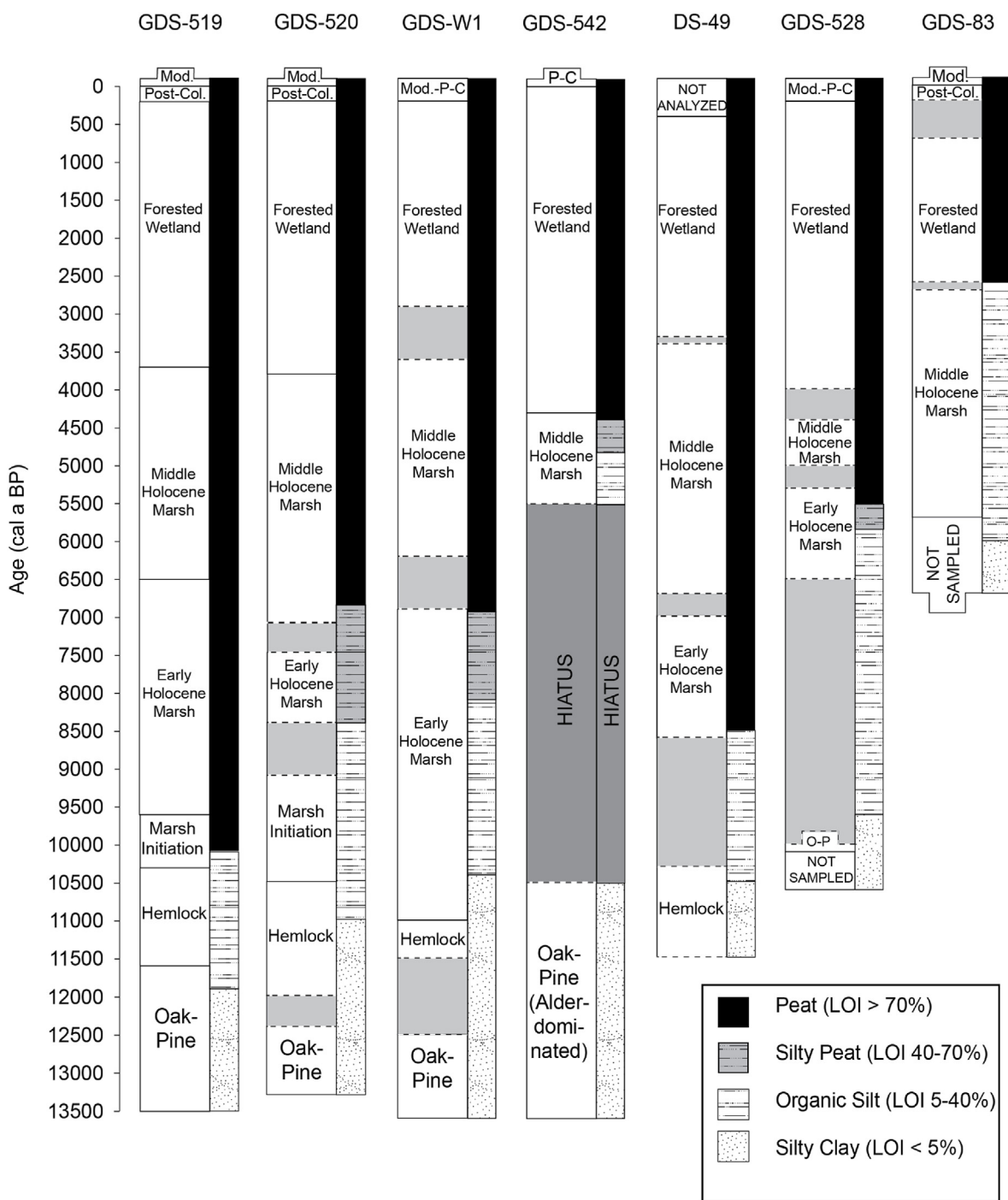

Fig. 4. Timing of vegetation changes at seven sites across Great Dismal Swamp NWR. Gray bands with dashed boundaries indicate intervals with uncertainty on timing of change due to lower sample resolution. No Loss-on-Ignition data are available for DS-49, so lithologic boundaries are based on descriptions in Whitehead (1972), and the age model was calculated using uncalibrated dates therein.

and 4). Future, higher-resolution sampling of the other sites could help to determine if the marsh initiation zone occurred elsewhere in the area.

3.3.4. Early Holocene marsh zone (9.6- ~6.5 cal ka BP)

The base of the Early Holocene marsh zone is characterized by the first consistent occurrence of *Carya* and *Liquidambar* and dominance of *Quercus* pollen (Fig. 3), representing the establishment of oak-hickory forests in upland forests adjacent to GDS. Marsh taxa, including Poaceae, *Typha*, *Sagittaria*, *Nymphaea,* and Asteraceae are common in this zone, and dominance of herbaceous plant macrofossils (Fig. 3) indicates the presence of non-woody marsh vegetation. Identifiable macrofossils are rare in this interval, but *Carex* and *Potamogeton* seeds are present near the top in GDS-W1 (Supplemental Fig. 2). Organic content increased in this zone, with sediments ranging from silty peats (LOI 40−70%) to "true" peats (LOI>70%) (Fig. 4). Pollen concentrations typically exceed 1,000,000 grains g^{-1}, and charcoal is consistently present at low levels (10−40 particles cm^{-2} yr^{-1} (Fig. 3, Supplemental Fig. 2). The age of the upper boundary of this zone is variable among the sites, with an upper boundary of ~6.5 cal ka BP at site GDS-519 and ~7.2 cal ka BP at site GDS-520, and 6.7 cal ka BP at site GDS-W1 (Fig. 3). The diachroneity of the boundary may be due to differences in elevation of the underlying Poquoson Member, which influenced water-table levels at the sites.

3.3.5. Middle Holocene marsh zone (~6.5 cal ka BP − 3.7 cal ka BP)

Continued dominance of *Quercus* pollen is consistent with persistence of oak-hickory forests in adjacent uplands, and increased abundance of *Pinus* pollen represents its expansion into nearby forests. *Nymphaea* pollen is less abundant in this zone, but *Sphagnum* and fern spores are common, as are pollen grains of other marsh taxa, including Poaceae, Asteraceae, Cyperaceae, and *Orontium*. Combined with dominance of herbaceous plant macrofossils, these assemblages indicate presence of marsh vegetation during this zone. Macrofossils of *Cyperus*, *Carex*, *Eleocharis parva*, and *Schoenoplectus americanus* are present, with occasional occurrence of *Eupatorium*, *Nymphaea odorata*, and *Taxodium distichum*. Cupressaceae pollen is present throughout the zone, with increased abundance in the uppermost samples. Charcoal abundance is greater in this zone, peaking at >400 particles cm^{-2} yr^{-1} in GDS-520, >1200 particles cm^{-2} yr^{-1} in GDS-519, and 110 particles cm^{-2} yr^{-1} in GDS-W1, with a small, but notable peak at GDS-542 (Fig. 3, Supplemental Figs. 1 and 2). Pollen concentrations typically range from 1 to 3 million grains g^{-1}, with lower concentrations over some intervals. At most sites, this zone is characterized by well-consolidated, humic peats with LOI ranging from near 80% at the base to 95% at the top of the zone. Site GDS-83 stands in contrast to the other sites, with the marsh zone persisting until 2.7 cal ka BP, LOI <20%, and rare occurrence of charcoal (Supplemental Fig. 3).

3.3.6. Forested Wetland zone (3.7−0.15 cal ka BP)

Nyssa and Cupressaceae pollen dominate this zone, collectively comprising >25% of assemblages, and the dominant species varies with location in the swamp. *Quercus* pollen abundance is halved, and continued presence of common *Pinus* pollen indicates establishment of the southeastern evergreen forests near the GDS wetland. *Ilex* and *Acer* pollen are common, and Ericaceae, *Morella*, and Polypodiaceae abundances are greater than in lower zones. *Sphagnum* is locally abundant. *Chamaecyparis* leaves were identified at two intervals at GDS-519. Much of this zone consists of highly organic (LOI>95%), well-consolidated peats, but more poorly consolidated peats with a "coffee-grounds" appearance occur in the upper 10−50 cm of the zone, depending on site location. Pollen

concentrations are high, usually exceeding 2 million grains g^{-1}. Charcoal is rare in the *Nyssa*-Cupressaceae zone, aside from site GDS-83, which differs from all other sites in the later onset (2.7 cal ka BP) of forested wetlands and increased charcoal concentrations after peat initiation (Supplemental Fig. 3). While charcoal concentrations are greater than in lower zones at site GDS-83, charcoal accumulation rates remain low (<15 particles cm^{-2} yr^{-1}). Charcoal also increased in GDS-542 between c. 2-1 cal ka BP but accumulation rates remain comparatively low (~20 particles cm^{-2} yr^{-1}), and a peak with similar timing (1.3−1.1 cal ka BP) is evident at GDS-528 (~260 particles cm^{-2} yr^{-1}) (Supplemental Figs. 1 and 4). A peak of >100 particles cm^{-2} yr^{-1} occurs at 0.21 cal ka BP at GDS-542.

3.3.7. Post-Colonial zone (0.15−0 cal ka BP)

The primary pollen signature of the post-Colonial zone is increased abundance of *Ambrosia*, typically accompanied by decreases in abundance of *Nyssa* and/or Cupressaceae pollen. The peat is poorly consolidated with a "coffee grounds" texture, pollen concentrations range from 1 to 5 million grains g^{-1}, and charcoal is rare.

3.3.8. Modern zone (0 cal ka BP − present)

The uppermost zone is characterized by sharp increases in abundance of *Acer* pollen, although there is considerable variability in abundance of other taxa among sites. Site GDS-528, which was collected in a site that underwent severe burns in 2008 and 2011 CE, exhibits an initial peak in *Acer*, followed by a near total loss of Cupressaceae pollen, a peak in *Eupatorium,* and a subsequent recovery of Cupressaceae and *Morella* pollen (Supplemental Fig. 4). Site GDS-519, the site least affected by ditching, shows only minor changes in pollen assemblages and doubling of *Acer* abundance. Site GDS-520 exhibits a significant increase in *Acer* pollen, followed by increases in Cupressaceae (Fig. 3b). Sample resolution at sites GDS-542 and GDS-W1 currently is inadequate to provide a detailed record of this time interval, but *Pinus* pollen abundance increases sharply in the uppermost two samples at GDS-542, indicating a shift to *Pinus* dominance in recent years (Supplemental Fig. 1). Future higher-resolution analyses could help to clarify the impacts of changes since the mid-20th century. Charcoal accumulation rates are highest of the Holocene record at site GDS-83, GDS-542, and GDS-528 and are elevated above the Post-Colonial zone levels at GDS-520. Poor recovery at the top of GDS-519 prevented analysis of charcoal in the modern zone.

3.4. Statistical analyses of pollen data

Detrended correspondence analysis of assemblage data from GDS surface samples shows that the primary driver of differences along the first axis is the combined abundance of taxa favoring longer hydroperiods and deeper water (*Nyssa* and Cupressaceae) versus more mesic taxa (including *Pinus*, *Ilex*, *Liquidambar*, *Acer,* and *Quercus*) (Supplemental Fig. 7). The second axis is controlled by the relative abundance of *Nyssa* vs. Cupressaceae pollen.

Comparison of fossil pollen assemblages from every sample in six cores using UPGMA cluster analysis highlights common patterns among the different sites. The unique *Alnus*-dominated assemblages from basal samples at GDS-542, *Pinus-Picea* forests, and Poaceae-dominated marshes of the late deglacial period each are separated into distinct clusters (Supplemental Fig. 9). The remaining two clusters consist of early to mid-Holocene samples representing cold-temperate forest and marsh assemblages and late Holocene forested wetlands dominated by *Nyssa* and Cupressaceae pollen.

3.5. Modern analogs for Great Dismal Swamp pollen assemblages

Monte Carlo resampling identifies an optimum squared chord distance (SCD) threshold of 0.18 to discriminate between analog and no-analog fossil-pollen assemblages, with the vegetation and depositional history of the GDS cores supporting this threshold. Depositional setting emerges as a key control on minimum SCD with most pollen assemblages from the GDS cores matching to modern analogs, although pre-Holocene samples have higher SCD values, with minima of approximately 0.18. Pollen assemblages before about 12 cal ka BP constitute a mixed forest of coniferous (*Picea*, *Pinus*) and hardwood taxa (*Quercus* and *Fagus* in Pine-Oak and Hemlock zones) which are characteristic of "no-analog" assemblages found throughout eastern North America during this interval (Williams et al., 2001). These mixed forests are poorly represented in the NAMPD, leading to higher dissimilarity in the pre-Holocene than the mid-to late-Holocene (Fig. 5e), and the interval coincides with deposition of clastic materials by stream flow prior to marsh initiation at c. 10.3 to 9.6 cal ka BP. These two confounding issues lead to higher dissimilarity values in the pre-Holocene and increase uncertainty in climatic reconstructions. However, the abundance of cold-adapted taxa (*Picea*, *Pinus*, *Alnus*, *Abies*, and *Betula*) in the Pine-Oak and Hemlock zones supports the reconstructed cool and mesic conditions (Figs. 3 and 7) (Thompson et al., 1999a,b). Indeed, the nearest analogs are located in Minnesota, Wisconsin, and Indiana which are defined by cold winters and warm summers.

The early Holocene (11.7 − c. 9.6 cal ka BP) is characterized by marsh initiation and Poaceae-dominated vegetation assemblages with minimum SCD values between 0.1 and 0.2. Similarly high Poaceae assemblages are common in the NAMPD for sites that reflect land-management practices in the southeastern United States (Whitmore et al., 2005), with most analogs located in farmlands throughout Georgia and North Carolina. Although minimum SCD values for these fossil-pollen assemblages are below the optimum threshold and those from the pre-Holocene samples, we exclude these individual assemblages from average climate reconstructions in light of the confounding effects of land management which obscure the role of climatic controls. Closest analogs for early to middle Holocene marsh zones were identified from lakes in North Carolina, South Carolina, and Georgia, resulting in higher than average Holocene MTWA reconstructions for that time interval. The differences in depositional setting between the analogs (lakes) and fossil assemblages (wetlands) highlights the fact that the analog calculations were driven primarily by regional and extralocal taxa, rather than the local marsh vegetation used to interpret patterns of wetland development. Following the marsh zones, modern pollen samples from the GDS area are the nearest analogs most frequently, with minimum SCD averaging 0.08, suggesting good analog matches, and represent the closest analogs throughout all the GDS cores. Notably, no other sites from the NAMPD match as analogs within these zones because of an underrepresentation of wetlands in the NAMPD.

3.6. Comparison of pollen-based paleoclimate reconstructions with TraCE-21 k model

Our pollen-based reconstructed temperature and precipitation time series compare well in broad terms to the TraCE-21 k simulation in the Holocene. Reconstructed MAT is largely stable after 8 cal ka BP, whereas the model displays a mild warming trend after 8 cal ka BP (Fig. 5a). Summer temperature peaks between 7 and
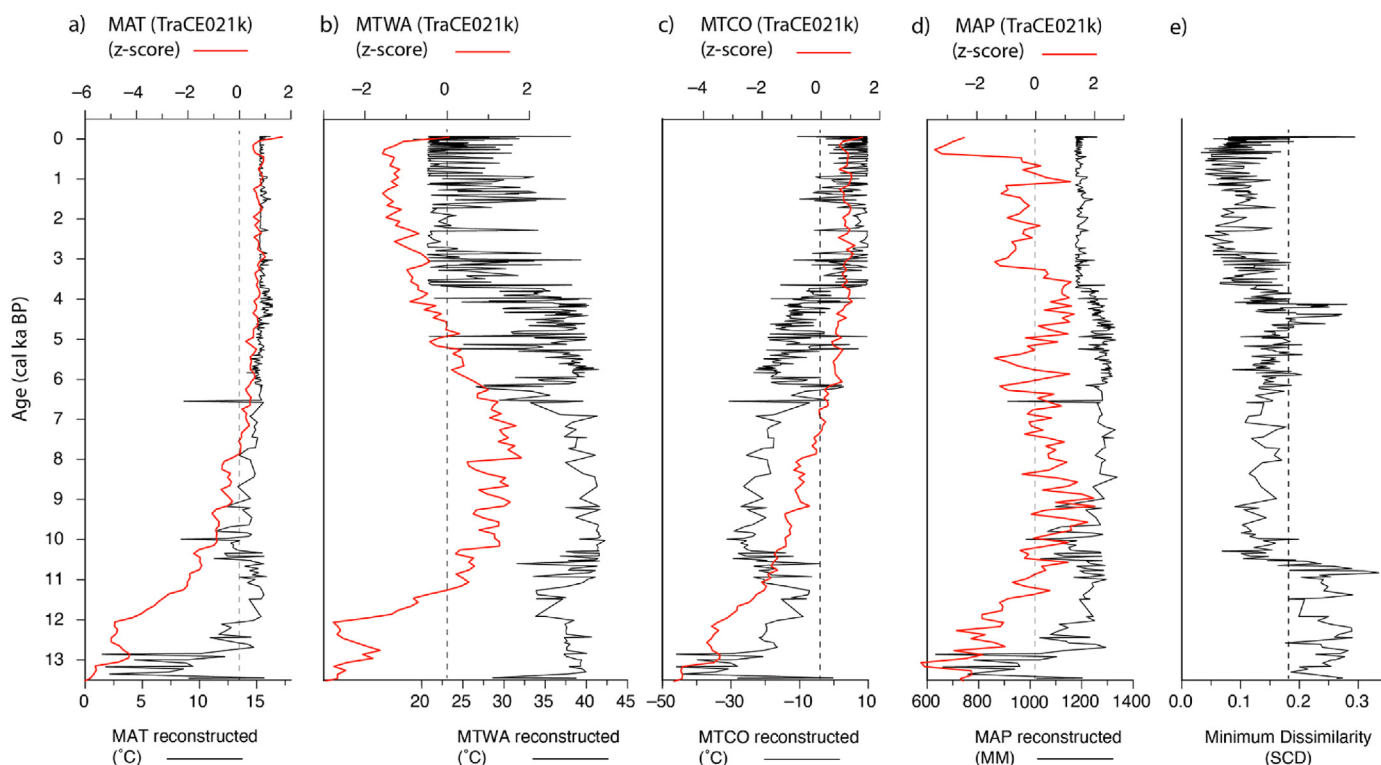

Fig. 5. Comparison of pollen-based paleoclimate reconstructions (black lines) with TraCE-21 k model runs (red lines) for the region. Dashed lines in a) MAT (mean annual temperature), b) MTWA (mean temperature warmest month), c) MTCO (mean temperature coldest month), and d) MAP (mean annual precipitation) figures represent Holocene means from TraCE-21 k model, and z-scores are centered on this mean. Most Holocene minimum dissimilarity values (squared chord distance) are less than the critical value of 0.18 indicated by the dashed line in panel e (see text for discussion).

9 cal ka BP in the TraCE-21 k simulation, which is not seen in the GDS reconstructed data, and both data and model display a summer cooling trend from the mid to late-Holocene (Fig. 5). TraCE-21 k simulates a gradual MTCO warming through the Holocene, whereas the data display a more abrupt warming between 6 and 3 cal ka BP. Data and model agreement is less clear for MAP due to the differing scales of variability and the influence of rising sea level on water table level, but TraCE-21 k simulates wetter-than-present conditions in the mid-Holocene, in agreement with the GDS reconstruction. Notably, the TraCE-21 k simulation also indicates decreased precipitation between c. 7 cal ka BP and 5 cal ka BP, coincident with the shift to shorter hydroperiod marshes and higher concentrations of charcoal.

4. Discussion

4.1. Mid-atlantic vegetation, climate, and fire at the Pleistocene-Holocene transition

During the late deglacial, from at least 13.5−11.7 cal ka BP, silty clays with low organic content were deposited along streams and adjacent floodplains in GDS, preserving pollen records of cold-temperate forests that grew in the area (Fig. 4). Oak-pine forests, including *Picea*, *Pinus banksiana* and *Abies,* occurred in the uplands, and *Fagus* was locally abundant, as documented at site GDS-519 (Fig. 3a). The abundance of *Fagus* at this low-elevation site near a stream may reflect locally greater water availability, as *Fagus* requires substantially more moisture than eastern pines and spruces (Burns and Honkala, 1990; Thompson et al., 1999a, 1999b). High abundance of *Alnus* pollen (up to 80%) at two eastern sites [GDS-542 (this study) and DS-77 (Whitehead, 1972)] (Supplemental Figs. 1 and 6) suggests that alder thickets lined streams in the eastern part of the study area. The rarity of charcoal during this period indicates low fire activity. No consistent changes in vegetation were noted in the Younger Dryas (YD) interval (12.9−11.7 cal ka BP), although the abundance of cool temperate taxa (*Pinus banksiana*-type*, Picea,* and *Fagus*) began a progressive decrease in the mid-YD that roughly parallels the warming trend indicated by oxygen isotopes from the NGRIP ice-core record (Fig. 6) and regional temperature reconstructions (Fastovich et al., 2020).

Comparison of fossil and modern assemblages found few close analogs prior to c. 10 cal ka BP, with most dissimilarity coefficients exceeding 0.25. This resulted, at least in part, from the lack of representation of similar depositional settings in the modern database, which consists primarily of lacustrine sites. Although the lack of close analogs makes the absolute values of reconstructions questionable, the fossil-pollen assemblages indicate that substantially cooler and drier than modern climates characterized the mid-Atlantic region during the late deglacial interval (Fig. 5). These estimates are consistent with the TraCE-21 k simulation for this time period, when the Laurentide Ice Sheet had a significant influence on atmospheric circulation patterns. These no-analog assemblages represent a unique mix of conifer and hardwood taxa that developed during the transition from glacial to interglacial conditions, as documented at numerous other sites in the eastern United States, including White Pond, South Carolina, Cupola Pond, Missouri, and Silver Lake, Ohio (Jones et al., 2017; Krause et al., 2018; Swisher and Peck, 2020).

The earliest Holocene assemblages (11.7−10.3 cal ka BP) are characterized by locally greater abundances of *Tsuga* and *Alnus*, representing their greater abundance in the uplands (Fig. 4). At the lowest elevation sites (GDS-519, GDS-520, GDS-W1, and DS-49), increased organic content and greater abundance of marsh pollen, including grasses and sedges, and dominance of herbaceous plant macrofossils, indicate the establishment of riparian marshes in the western parts of the refuge (Fig. 3, Supplemental Fig. 5). In eastern sites (GDS-542 and GDS-W1), the continued occurrence of common *Alnus* indicates persistence of floodplain thickets into the earliest Holocene (Supplemental Figs. 1 and 2).

4.2. Early to mid-Holocene wetland development in Great Dismal Swamp

As early as 10.3 cal ka BP, grass-dominated marshes, characterized by Poaceae pollen abundance exceeding 40% and dominance of herbaceous plant macrofossils, were established along the lowest elevation stream courses (sites GDS-519 and -520: Fig. 4), where they persisted until c. 9.2 cal ka BP. A possible analog could be modern "cane" (*Arundinaria*) thickets, which grow on slightly elevated ridges in alluvial floodplains, tolerate periodic inundation (Delcourt, 1976; Platt and Brantley, 1997), and require fires every 3−5 years to maintain healthy stands (Wells, 1942; Hughes, 1966). However, the high abundance of grass pollen in the GDS samples is suggestive that GDS grasses were not the woody *Arundinaria*, which is semi-semelparous and flowers every 4−25 years (Triplett et al., 2010). The co-occurrence of grass-dominated vegetation with modest increases in charcoal content (Fig. 6) indicates that wildfires were common in these floodplain marshes. Marsh establishment along these low-lying streams may have been facilitated by increases in groundwater levels related to rapid early Holocene rates of sea-level rise (6.4 mm yr^{-1} from 11 to 10 cal ka BP: Cronin et al., 2019). Additional evidence for elevated water tables lies in accumulation of true peats (LOI>70%) as early as 10 cal ka BP at the low-elevation site GDS-519 and organic silts (LOI 5−40%) at slightly higher elevation sites including GDS-520, GDS-W1, GDS-528, and DS-49 b y c.10 cal ka BP (Fig. 4).

By c. 9.6 cal ka BP, GDS hydroperiods lengthened enough to support peat-accumulating marshes (>70% organic matter) with floating aquatics such as *Nymphaea* and *Nuphar* at the lowest elevation sites and transitions to silty peats at GDS-520 and GDS-W1. These long-hydroperiod marshes persisted until 6−7 cal ka BP (Fig. 4) and correspond to an interval of increased MAP (Fig. 5d). Additionally, a rapid rise in sea level (3.0−5.8 mm yr^{-1} from 9 to 6 cal ka BP: Cronin et al., 2019; Ramsey et al., 2022) may have influenced the water table. Modeling and field efforts have shown that sea-level rise directly influences elevation of groundwater (Bjerklie et al., 2012) and the area affected by flooding (Rotzoll and Fletcher, 2013), and our results suggest that water-table response to rapid deglacial sea-level rise (11.0−12.5 m from 9 to 6 cal ka BP: Cronin et al., 2019; Ramsey et al., 2022) may have combined with increased precipitation to facilitate development of freshwater wetlands in this site on the outer Coastal Plain. Dominance of *Quercus* and *Carya* pollen indicates that oak-hickory forests were established in adjacent uplands while the peat- and silty-peat accumulating marshes were established along stream courses in GDS.

By 6−7 cal ka BP, peat was accumulating across most of the modern GDS (Whitehead, 1972), and organic silts were accumulating at site GDS-83 (Fig. 4). Shorter-hydroperiod marshes, characterized by Cyperaceae, Asteraceae, *Orontium*, ferns, and other marsh taxa, were established between 6.5 and 7 cal ka BP, reflecting the increasing elevation of the peat surface, decreased MAP (Fig. 5e), and slower rates of sea-level rise (4−5 mm yr^{-1}: Cronin et al., 2019; Ramsey et al., 2022). Regionally, evidence for a drier mid-Holocene is provided by higher oxygen isotope ratios in West Virginia speleothems (Hardt et al., 2010) and lower lake levels in
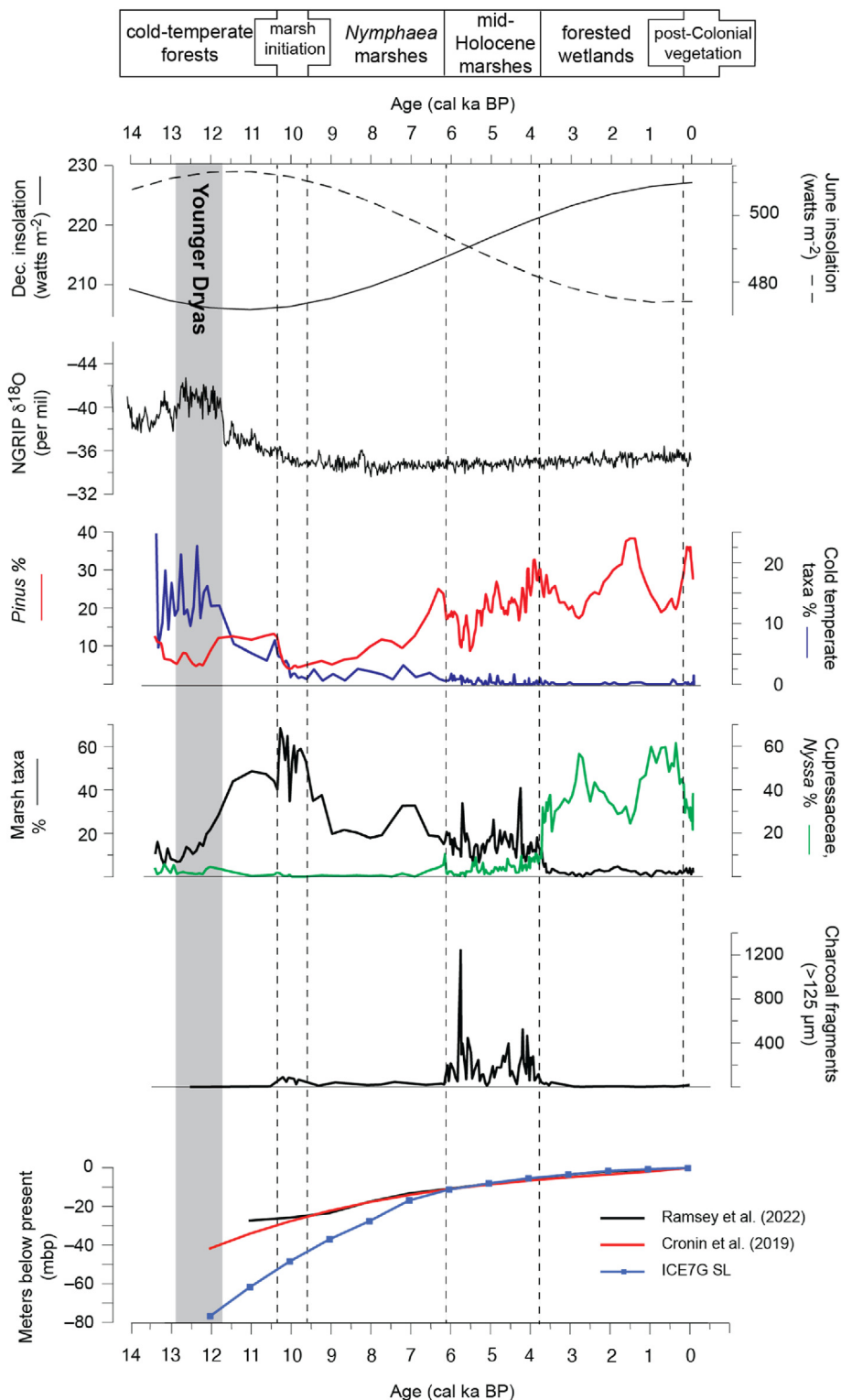
Fig. 6. Deglacial-Holocene record of vegetation and charcoal at GDS-519, compared to June and December insolation curves (30° N, Berger and Loutre, 1991), oxygen isotope curve from NGRIP ice core (Vinther et al., 2006; Rasmussen et al., 2006), sea-level data from Cronin et al. (2019) and Ramsey et al. (2022) relative to modeling predictions based on the ICE-7G_NA (VM7) model of Roy and Peltier (2018). The cold-temperate forest zone corresponds to the Oak-Pine and Hemlock zones. Cold temperate taxa include *Abies*, *Picea*, and *P. banksiana*-type. Marsh taxa include Poaceae, Cyperaceae, Asteraceae, *Nymphaea*, *Nuphar*, *Sagittaria*, *Utricularia*, *Typha*, and ferns.

Massachusetts (Shuman et al., 2001) and South Carolina (Krause et al., 2018). These observations are consistent with TraCE-21 k reconstructions that indicate that a decrease in MAP to values lower than the Holocene mean between c. 7.4–5.9 cal ka BP (Fig. 5). Charcoal concentrations increased significantly during this interval (Fig. 6), indicating increased wildfire activity. Both pollen-based
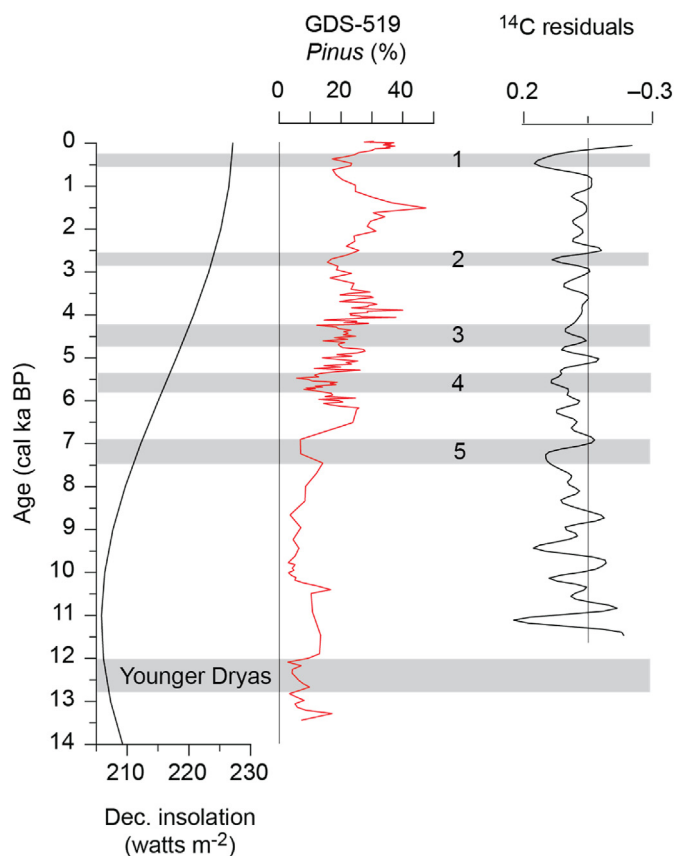
Fig. 7. The pollen record from site GDS-519 records millennial-scale variability in *Pinus* abundance throughout the Holocene. Increased abundance of *Pinus* pollen in Great Dismal Swamp parallels increasing winter insolation in the late Holocene (Berger and Loutre, 1991). *Pinus* minima, numbered 1–5, each lasted several hundred years and correspond to solar minima recorded by ^{14}C residuals (Bond et al., 2001).

and TraCE-21 k reconstructions indicate that MAT approached modern temperatures, with a progressive increase in MTCO paralleling increasing winter insolation (Fig. 6).

4.3. Late Holocene development of forested wetlands

Forested wetlands developed nearly synchronously across the GDS landscape at c. 3.7 cal ka BP with the exception of the higher-elevation site (GDS-83) (Fig. 1a). Forested wetland deposits all consist of peat (LOI>70%), and pollen assemblages are dominated by *Nyssa* and Cupressaceae pollen and are analogous to modern assemblages collected throughout GDS and forested wetlands along the nearby lower Roanoke River in North Carolina. Because it is difficult to distinguish *Taxodium* from *Chamaecyparis* pollen and identifiable needles were sparse, we cannot definitively determine the distribution of cypress-tupelo vs. Atlantic white cedar in these late Holocene swamps, but each is characterized by standing water and longer hydroperiods than the modern maple-gum swamps. *Acer*, *Ilex*, Ericaceae, *Sphagnum*, and polypodiaceous ferns were common elements of these swamps, and the assemblages remained relatively stable until land disturbances associated with European colonization altered vegetation in GDS and the surrounding areas in the late 1700s CE. Wildfires were uncommon in the forested wetlands, and the shift from oak-hickory to southeastern pine forests in nearby uplands is coincident with development of forested wetlands in GDS.

Differences in relative abundance of Cupressaceae and *Nyssa*

pollen exist among the sites and likely are related to local hydrologic differences. Late Holocene assemblages at the lowest elevation site most proximal to a paleostream (GDS-519), are strongly dominated by *Nyssa* pollen, whereas the nearby, higher elevation site GDS-520 is dominated by Cupressaceae pollen (Fig. 3). This is consistent with observations of modern *Nyssa* showing that it is more competitive than *Taxodium* under continuous flooding and higher water tables (Brown, 1981; Dicke and Toliver, 1990; Keeland and Sharitz, 1995), and that shallower, more variable flooding favors growth of *Taxodium* (Keeland et al., 1997). Likewise, *Chamaecyparis thyoides* forests typically thrive in settings with variable hydroperiods and seasonal drying (Laderman, 1989), so Cupressaceae dominance is indicative of shallower, more variable flooding than those dominated by *Nyssa*.

The shift from marshes to forested wetlands c. 3.7 cal ka BP coincides with a 50% reduction in rates of post-glacial sea-level rise between 4 and 3 cal ka BP (Cronin et al., 2019; Ramsey et al., 2022) (Fig. 6). The stabilization of rates of sea-level rise also may have slowed rates of water table rise, and the subsequent shortening of hydroperiod, combined with increased peat accumulation and surface elevation, appear to have been sufficient for replacement of the marsh by a forested wetland. This is likely akin to the fen-bog transition described in northern peatlands, as the forested wetlands today are oligotrophic, similar to forested bogs (Treat et al., 2021). The minor-but-consistent increased abundance of Cupressaceae pollen in the mid-Holocene marsh zone is suggestive of the gradual lowering of the water table and increased seasonality of inundation during the middle Holocene. Combined with a change in precipitation seasonality (Shuman and Donnelly, 2006), these factors facilitated establishment of the forested wetland in GDS.

4.4. Anthropogenic impacts on Great Dismal Swamp

Cores collected throughout GDS show both regional and local impacts of land clearance during the last few centuries. Although direct impacts of colonial land clearance in GDS were minor compared to those in lacustrine and estuarine sites (Brush, 1984; Willard et al., 2003), the GDS wetlands preserve records of clearance in nearby uplands through an increased abundance of *Ambrosia* pollen (0.15 cal ka BP) (Fig. 3, Supplemental Figs. 1–4). The more localized impacts of ditching that began as early as 1763 CE, are evident in pollen assemblages from each study site. Analysis of vegetational patterns in sediment cores collected across GDS indicates that modern distribution of vegetation in the wetland primarily is the result of hydrologic differences related to wetland drainage. This highlights the fact that anthropogenic factors may play a larger role than climate in influencing modern wetland vegetation, adding to the uncertainty associated with the use of wetland assemblages to reconstruct past climate. It is worth noting, however, that the over-arching signature of adjacent upland vegetation is preserved in these wetland records, providing an overview of both local and regional vegetation.

4.4.1. Colonial-era land clearance and ditching

The earliest well-dated impacts of ditching are seen at GDS-83, located west of Jericho Ditch, which was built in 1810 CE to transport both shingles and tourists taking gondola rides into the swamp (Trout, 2004). A halving of *Pinus* and accompanying increase in *Ambrosia* pollen abundance is correlated with forest clearance in the uplands. This shift also is accompanied by a shift from *Nyssa* to Cupressaceae pollen dominance, which may reflect lowering of the water table as water was drained from the site by the Jericho Ditch. The impacts of logging near Jericho Ditch were noted as early as 1934 CE by Cocke et al. (1934), who observed the presence of second growth trees and evidence of cutting at sites 12 and 14 (Fig. 1a),

as well as the loss of *Taxodium* pollen in the uppermost sample of a core collected at site 14.

Sites east of the Dismal Swamp Canal, which began construction in 1793 CE and underwent numerous expansions since then, were analyzed both by Lewis and Cocke (1929) and Whitehead (1972). Although no radiocarbon dates are available for either site, the dominance of *Quercus* pollen in the upper samples of Whitehead's site DS-77 (Supplemental Fig. 6), collected directly east of Dismal Swamp Canal in the early 1960s, is suggestive of the absence of late Holocene sediments. Comparison of recounts of the original DS-77 samples with modern samples indicates that the upper part of that core bears little resemblance to assemblages characteristic of the modern maple-gum swamp that occupies the site, and it is likely that late Holocene sediments were lost due to disturbance, drainage, and oxidation of peats. Pollen assemblages from the Lewis & Cocke site, collected farther south in the 1920's, contained at least 35 cm of peat dominated by cypress and tupelo pollen, likely of late Holocene age (Supplemental Fig. 8). Although this site has yet to be revisited, it appears that construction of the canal and subsequent drainage in the 19th and 20th centuries may have caused substantial oxidation and loss of peat east of the Dismal Swamp Canal, and analysis of additional sites would address its role in peat oxidation and carbon dynamics.

4.4.2. Impacts of Mid-20th century ditching of Great Dismal Swamp

Most GDS ditches were constructed between 1950 and 1960 CE (Trout, 2004) for timber removal. Pollen evidence indicates that the resulting hydrologic changes had substantial effects on GDS vegetation, even at the least-affected site, GDS-519. At that site, located west of Sherrill Ditch, pollen assemblages showed a modest increase in *Acer, Liquidambar*, and *Ilex* pollen late in the 20th century, even though the site still occupied by cypress-tupelo swamp. Site GDS-520, located on the east side of Sherrill Ditch, currently is a maple-gum swamp, and pollen evidence indicates that the site was occupied by cypress-tupelo or Atlantic white cedar forest from c. 3.7 cal ka BP until ditch construction in the mid-20th century. Site GDS-83, already affected by 19th century ditching, underwent additional vegetation changes after construction of the Lynn Ditch west of the site in the mid-20th century. *Acer, Liquidambar*, and *Nyssa* pollen increased in abundance sharply (Supplemental Fig. 3), indicating expansion of maple-gum forests at the site. Likewise, pollen evidence indicates that Site GDS-542, located in pine pocosin forest east of Laurel Ditch on the east side of the Refuge, was occupied by a cypress-tupelo or Atlantic white cedar forest until ditch construction, when increased abundance of pine, maple, and sweetgum pollen (Supplemental Fig. 1) indicate a substantial change in forest composition. A similar pattern was noted in a core collected previously in pine pocosins (Stevens and Patterson, 1998), in which *Pinus* replaced Cupressaceae in dominance, tripling in abundance in the upper few centimeters of the core.

Ditching in peatlands can increase fire severity (Benscoter et al., 2011) by lowering the water table and altering site hydrology. In GDS, 20th century ditching may have influenced the frequency and severity of wildfires (Spieran and Wurster, 2020). Two major fires, in 2008 and 2011 CE, burned for months and resulted in conversion of 45 km² of forested wetland to marsh (Spieran and Wurster, 2020). The charcoal record from site GDS-528, collected within the burned zone, documents the occurrence of those fires and indicates that these modern fires were on par with or worse than the most severe fires of the mid-Holocene (Supplemental Fig. 4). Further high-resolution analysis of cores from other sites could help to document and understand the frequency and impact of fires across the wetland.

Collectively, these records indicate that the modern forest composition and distribution in Great Dismal Swamp is largely an artifact of more than two centuries of ditching, logging, and changes to the natural hydrology. For at least the previous two millennia, most of Great Dismal Swamp was covered by a mix of cypress-tupelo and Atlantic white cedar swamps, which were largely replaced by maple-gum and, to a lesser extent, pine-dominated swamp forests.

4.5. Regional changes in climate and vegetation from Great Dismal Swamp records

Although wetland records from GDS primarily record local changes in vegetation and hydrology, the abundance of pollen from upland taxa allows them to provide insights into climate-driven shifts in regional forests. Holocene records from lake and estuarine deposits in the Atlantic Coastal Plain are characterized by a shift from early Holocene dominance of *Quercus* to *Pinus* pollen dominance in the late Holocene (Krause et al., 2018; Spencer et al., 2017; Watts, 1979; Willard et al., 2005), and this shift also is evident in records from the GDS wetlands and other wetland deposits in North Carolina and Georgia (Goman and Leigh, 2004; LaMoreaux et al., 2009). Previous studies have suggested that warmer winters associated with increasing winter insolation in the late Holocene drove the northward expansion of southern pines along the Coastal Plain (Watts, 1979; Willard et al., 2005), and the increasing abundance of *Pinus* pollen in the late Holocene roughly parallels increasing December insolation in mid-latitudes (Fig. 6). The pine forests that occupy large swaths of the Atlantic Coastal Plain of North Carolina and Virginia (Braun, 1950) are dominated by *Pinus echinata, P. elliottii, P. palustris, P. taeda*, and *P. virginiana*, which require warmer winters (> −5.9 °C) and greater moisture availability (>885 mm annual precipitation) than northeastern pines, which can tolerate winter temperatures as cold as −30 °C with as little as 250 mm annual precipitation (Iverson et al., 1999; Thompson et al., 2000). Reconstructed winter temperatures (Fig. 5) from GDS and model simulations both indicate progressive mid-to late-Holocene winter warming, which is consistent with the hypothesis that southern *Pinus* expansion resulted from increasing winter insolation in the late Holocene.

The high-resolution record of *Pinus* pollen in GDS sediments also illustrates millennial-scale variability that is consistent with that identified in previous studies (Bond et al., 2001; Wanner et al., 2011; Willard et al., 2005). Five pine minima were identified from GDS-519, centered at 0.6, 2.9, 4.2, 5.4, and 7.1 cal ka BP that lasted approximately 300−500 years each (Fig. 7). Based on documented correlations between the abundance of *Pinus* pollen, mean January temperature, and, to a lesser extent, mean annual precipitation (Willard et al., 2005), we interpret these pine minima as representing multidecadal to centennial-scale intervals characterized by cooler, drier winters that affected forest composition on the unconsolidated Coastal Plain soils west of Great Dismal Swamp. Although the influence of these quasi-periodic intervals is most evident in late Holocene sediments from GDS (Fig. 7), they have been identified throughout the Holocene in Chesapeake Bay sediments and appear to be correlated with solar minima recorded by both ¹⁴C residuals and the Be record from NGRIP (Bond et al., 2001; Willard et al., 2005), as well as with late Holocene cooling events identified by Wanner et al. (2011). This highlights the utility of wetland pollen records to reconstruct both localized fluctuations in hydrology and regional forest response to larger-scale climate change.

5. Conclusions

Sediments underlying GDS preserve a record of vegetational change in both the wetland itself and adjacent upland forests

during the last 13,500 years, as well as the fire history of the wetland. During the late deglacial, from 13.5 cal ka BP through the YD, cold temperate forests occupied uplands near GDS, and they were replaced by oak-hickory forests as the Laurentide Ice Sheet retreated and temperatures warmed in the early Holocene. In GDS, riparian wetlands, dominated by grasses, were established along the lowest-elevation stream banks in the early Holocene, with peat accumulation beginning in the lowest elevation site at c.10 cal ka BP. The grass-dominated marshes were succeeded by longer-hydroperiod marshes as early as 9.6 cal ka BP, as rapid rates of sea-level rise and increased precipitation combined to raise the water table and flood the low-lying GDS area sufficiently for wetland development. By 7-6 cal ka BP, sufficient thicknesses of organic material accumulated that "true" peats blanketed most of the GDS landscape, and a combination of slowing rates of sea-level/water-table rise, increasing peat elevation, and drier middle Holocene climates resulted in expansion of shorter-hydroperiod, fire-prone wetlands across the landscape. Replacement of oak-hickory forests by pine-oak forests in the uplands was accompanied by establishment of forested wetlands across most of the GDS landscape at c. 3.7 cal ka BP, when rates of sea-level and water-table rise slowed. These cypress-tupelo and Atlantic white cedar swamps persisted until hydrologic changes from ditch construction, starting in the late 18th century and peaking in the mid-20th century, resulted in expansion of the maple-gum and pine pocosin forests that dominate the modern Great Dismal Swamp landscape. Collectively, these records document the combined impacts of deglacial warming, sea-level rise, Holocene climate variability, and anthropogenic land cover change in local wetlands and regional forests of the mid-Atlantic Coastal Plain in North America.

Author contributions

Debra Willard: Conceptualization, Methodology, Investigation, Formal Analysis, Data Curation, Writing — Original Draft; Miriam Jones: Conceptualization, Methodology, Investigation, Formal Analysis, Writing — Review & Editing; Jay Alder: Software, Writing — Review & Editing; David Fastovich - Software, Writing — Review & Editing; Kristen Hoefke — Investigation; Robert Poirier - Writing — Review & Editing; Frederic Wurster — Investigation, Writing — Review & Editing.

Declaration of competing interest

The authors declare that they have no known competing financial interests or personal relationships that could have appeared to influence the work reported in this paper.

Data availability

Data are reposited at www.neotomadb.org and https://www.ncei.noaa.gov. Code for analogs and paleoclimate reconstructions are available at https://github.com/davidfastovich/gds_climate_reconstruction.

Acknowledgments

Appendix A. Supplementary data

Supplementary data to this article can be found online at https://doi.org/10.1016/j.quascirev.2023.108153.

References

Abernethy, Y., Turner, R.E., 1987. US forested wetlands: 1940-1980: field-data surveys document changes and can guide national resource management. Biosci 37, 721–727. https://doi.org/10.2307/1310469.

Barak, R.S., Hipp, A.L., Cavender-Bares, J., Pearse, W.D., Hotchkiss, S.C., Lynch, E.A., Callaway, J.C., Calcote, R., Larkin, D.J., 2016. Taking the long view: integrating recorded, archeological, paleoecological, and evolutionary data into ecological restoration. Int. J. Plant Sci. 177, 90–102. https://doi.org/10.1086/683394.

Bartlein, P.J., Harrison, S.P., Brewer, S., Connor, S., Davis, B.A.S., Gajewski, K., Guiot, J., Harrison-Prentice, T.I., Henderson, A., Peyron, O., Prentice, I.C., Scholze, M., Seppä, H., Shuman, B., Sugita, S., Thompson, R.S., Viau, A.E., Williams, J., Wu, H., 2011. Pollen-based continental climate reconstructions at 6 and 21 cal ka BP: a global synthesis. Clim. Dyn. 37, 775–802. https://doi.org/10.1007/s00382-010-0904-1.

Bazzaz, F.A., 1974. Ecophysiology of *Ambrosia artemisiifolia*, a successional dominant. Ecol. 55, 112–119. https://doi.org/10.2307/1934623.

Benscoter, B.W., Thompson, D.K., Waddington, J.M., Flannigan, M.D., Wotton, B.M., De Groot, W.J., Turetsky, M.R., 2011. Interactive effects of vegetation, soil moisture and bulk density on depth of burning of thick organic soils. Int. J. Wildland Fire 20, 418–429. https://doi.org/10.1071/WF08183.

Berger, A., Loutre, M.F., 1991. Insolation values for the climate of the last 10 million years. Quat. Sci. Rev. 10, 297–317. https://doi.org/10.1016/0277-3791(91)90033-Q.

Bjerklie, D.M., Mullaney, J.R., Stone, J.R., Skinner, B.J., Ramlow, M.A., 2012. Preliminary investigation of the effects of sea-level rise on groundwater levels in New Haven, Connecticut. U.S. Geol. Surv. Open-File Rep. 2012–1025, 46. http://pubs.usgs.gov/of/2012/1025/.

Blaauw, M., Christen, J.A., 2011. Flexible paleoclimate age-depth models using an autoregressive gamma process. Bayesian Anal 6, 457–474. https://doi.org/10.1214/11-BA618.

Blanton, D.B., 2002. Dismal swamp prehistory as represented by the magnolia site, Suffolk, Virginia. Q. Bull. Archeol. Soc. Virginia 57, 38–48.

Blanton, D.B., 2003. Late Archaic in Virginia: an updated overview. Q. Bull. Archeol. Soc. Virginia 58, 177–206.

Bond, G.C., Kromer, B., Beer, J., Muscheler, R., Evans, M.N., Showers, W., Hoffmann, S., Lotti-Bond, R., Hajdas, I., Bonani, G., 2001. Persistent solar influence on North Atlantic climate during the Holocene. Science 294, 2130–2136. https://doi.org/10.1126/science.1065680.

Bottoms, E.E., 1983. Seventeenth Century Settlement of the Nansemond River in Virginia. Master of Arts (MA), Thesis, History. In: Braun, E.L., 1950. Deciduous Forests of Eastern North America. The Blakiston, Philadelphia. Old Dominion University, Norfolk, Virginia. https://doi.org/10.25777/9ppr-2744.

Bottoms, E., Painter, F., 1979. Evidence of aboriginal utilization of the bola in the Dismal Swamp area. In: Kirk Jr., P.W. (Ed.), The Great Dismal Swamp. University Press of Virginia, Charlottesville, Virginia, pp. 44–56.

Braun, E.L., 1950. Deciduous Forests of Eastern North America. The, Blakiston, Philadelphia.

Brown, S., 1981. A comparison of the structure, primary productivity, and transpiration of cypress ecosystems in Florida. Ecol. Monogr. 51, 403–427. https://www.jstor.org/stable/2937322.

Brown, T.A., Nelson, D.E., Mathewes, R.W., Vogel, J.S., Southon, J.R., 1989. Radiocarbon dating of pollen by accelerator mass spectrometry. Quat. Res. 32, 205–212. https://doi.org/10.1016/0033-5894(89)90076-8.

Brush, G.S., 1984. Patterns of recent sediment accumulation in Chesapeake Bay (Virginia-Maryland, U.S.A.) tributaries. Chem. Geol. 44, 227–242. https://doi.org/10.1016/0009-2541(84)90074-3.

Burns, R.M., Honkala, B.H., 1990. Silvics of North America: 1. Conifers; 2 Hardwoods. In: Hardwoods Agriculture Handbook 654. U.S. Dept. Agric., For. Serv., Washington, D.C.

Chevalier, M., Davis, B.A.S., Heiri, et al., 2020. Pollen-based climate reconstruction techniques for late Quaternary studies. Earth Sci. Rev. 210, 103384. https://doi.org/10.1016/j.earscirev.2020.103384.

Cocke, E.C., Lewis, I.F., Patrick, R., 1934. A further study of Dismal Swamp peat. Am. J. Bot. 21, 374–395. https://www.jstor.org/stable/2436376.

Cronin, T.M., Clevenger, M.K., Tibert, N.E., Prescott, T., Toomey, M., Hubeny, J.B., Abbott, M.B., Seidenstein, J., Whitworth, H., Fisher, S., Wondolowski, N., Ruefer, A., 2019. Holocene sea-level variability from Chesapeake Bay tidal marshes, USA. Holocene 29, 1679–1693. https://doi.org/10.1177/0959683619862028.

Dahl, T.E., Allord, G.J., 1996. Technical aspects of wetlands: History of wetlands in

the conterminous United States. In: Fretwell, J.D., Williams, J.S., Redman, P.J. (Eds.), National Water Summary on Wetland Resources. U.S. Geol. Surv. Water-Supply Paper 2425. U.S. Government Printing Office, Washington, D.C., pp. 19–26. https://water.usgs.gov/nwsum/WSP2425/history.html

Dean, W.E., 1974. Determination of carbonate and organic matter in calcareous sediments and sedimentary rocks by loss on ignition; comparison with other methods. J. Sediment. Res. 44, 242–248. https://doi.org/10.1306/74d729d2-2b21-11d7-8648000102c1865d.

Delcourt, H.R., 1976. Presettlement vegetation of the North of Red River Land District, Louisiana. Castanea 41, 122–139. https://www.jstor.org/stable/4032662.

Dicke, S.G., Toliver, J.R., 1990. Growth and development of bald-cypress/water-tupelo stands under continuous versus seasonal flooding. For. Ecol. Management 33/34, 523–530. https://doi.org/10.1016/0378-1127(90)90215-W.

Drexler, J.Z., Fuller, C.C., Orlando, J., Salas, A., Wurster, F.C., Duberstein, J.A., 2017. Estimation and uncertainty of recent carbon accumulation and vertical accretion in drained and undrained forested peatlands of the southeastern USA. J. Geophys. Res., Biogeosciences 122, 2563–2579. https://doi.org/10.1002/2017JG003950.

Egghart, C., 2020. State. Plan and research design Middle Archaic (6500 BC − 2500 BC). In: Moore, E.A., Means, B.K. (Eds.), The Archaeology of Virginia's First Peoples. The Archeological Society of Virginia, pp. 53–70.

Fastovich, D., Russell, J.M., Jackson, S.T., Krause, T.R., Marcott, S.A., Williams, J.W., 2020. Spatial fingerprint of Younger Dryas cooling and warming in eastern North America. Geophys. Res. Lett. 47 (22), e2020GL090031. https://doi.org/10.1029/2020GL090031.

Fowler, C., Konopik, E., 2007. The history of fire in the southern United States. Hum. Ecol. Rev. 14, 165–176. https://www.jstor.org/stable/24707703.

Goman, M., Leigh, D.S., 2004. Wet early to middle Holocene conditions on the upper Coastal Plain of North Carolina, USA. Quat. Res. 61, 256–264. https://doi.org/10.1016/j.yqres.2004.02.007.

Grimm, E.C., 1987. CONISS: a FORTRAN 77 program for stratigraphically constrained cluster analysis by the method of incremental sum of squares. Comput. Geosci. 13, 13–35. https://doi.org/10.1016/0098-3004(87)90022-7.

Hammer, Ø., Harper, D.A., Ryan, P.D., 2001. PAST: Paleontological statistics software package for education and data analysis. Palaeontol. Electron. 4, 9. http://palaeo-electronica.org/2001_1/past/issue1_01.htm.

Hammett, J.E., 1992. The shapes of adaptation: historical ecology of anthropogenic landscapes in the southeastern United States. Landsc. Ecol. 7, 121–135.

Hansen, B., 2010. Bogged Down − the Dismal Swamp Canal, vol. 5. Civil Eng., New York, pp. 46–49.

Hardt, B., Rowe, H.D., Springer, G.S., Cheng, H., Edwards, R.L., 2010. The seasonality of east central North American precipitation based on three coeval Holocene speleothems from southern West Virginia. Earth Planet Sci. Lett. 295, 342–348. https://doi.org/10.1016/j.epsl.2010.04.002.

Harris, I., Osborn, T.J., Jones, P., Lister, D., 2020. Version 4 of the CRU TS monthly high-resolution gridded multivariate climate dataset. Sci. Data 7, 109. https://doi.org/10.1038/s41597-020-0453-3.

Hughes, R.H., 1966. In: Fire ecology of canebrakes. Proceedings: 5th Tall Timbers Fire Ecology Conf., 5, pp. 149–258.

Hupp, C.R., 2000. Hydrology, geomorphology and vegetation of Coastal Plain rivers in the south-eastern USA. Hydrol. Process. 14, 2991–3010. https://doi.org/10.1002/1099-1085(200011/12)14:16/17<2991::AID-HYP131>3.0.CO;2-H.

Hurrell, J.W., 1995. Decadal trends in the North Atlantic Oscillation: regional temperatures and precipitation. Science 269, 676–679. https://doi.org/10.1126/science.269.5224.676.

Iverson, L.R., Prasad, A.M., Hale, B.J., Sutherland, E.K., 1999. Atlas of current and potential future distributions of common trees of the Eastern United States. U.S. Dept. Agric., For. Serv. Gen. Tech. Rep., NE-265, 1-245.

Jackson, S.T., Hobbs, R.J., 2009. Ecological restoration in the light of ecological history. Science 325, 567–569. https://doi.org/10.1126/science.1172977.

Jackson, S.T., Williams, J.W., 2004. Modern analogs in Quaternary paleoecology: Here today, gone yesterday, gone tomorrow? Annu. Rev. Earth Planet Sci. 32, 495–537. https://doi.org/10.1146/annurev.earth.32.101802.120435.

Jackson, S.T., Webb, R.S., Anderson, K.H., Overpeck, J.T., Webb III, T., Williams, J.W., Hansen, B.C.S., 2000. Vegetation and environment in eastern North America during the Last Glacial Maximum. Quat. Sci. Rev. 19, 489–508. https://doi.org/10.1016/S0277-3791(99)00093-1.

Janssen, C.R., 1984. Modern pollen assemblages and vegetation in the Myrtle Lake peatland, Minnesota. Ecol. Monogr. 54, 213–252. https://www.jstor.org/stable/1942662.

Jones, R.A., Williams, J.W., Jackson, S.T., 2017. Vegetation history since the last glacial maximum in the Ozark highlands (USA): a new record from Cupola Pond, Missouri. Quat. Sci. Rev. 170, 174–187. https://doi.org/10.1016/j.quascirev.2017.06.024.

Juggins, S., 2015. Rioja: Analysis of Quaternary science data. In: R Package Version (0.9-5), the Comprehensive R Archive Network.

Keeland, B.D., Sharitz, R.R., 1995. Seasonal growth patterns of *Nyssa sylvatica* var. *biflora, Nyssa aquatica*, and *Taxodium distichum* as affected by hydrologic regime. Can. J. For. Res. 25, 1084–1096. https://doi.org/10.1139/x95-120.

Keeland, B.D., Conner, W.H., Sharitz, R.R., 1997. A comparison of wetland tree growth response to hydrologic regime in Louisiana and South Carolina. For. Ecol. Management 90, 237–250. https://doi.org/10.1016/S0378-1127(96)03901-1.

Keever, C., 1983. A retrospective view of old-field succession after 35 years. Am. Midl. Nat. 110, 397–404.

King, S.L., Keim, R.F., 2019. Hydrologic modifications challenge bottomland hardwood forest management. J. Fr. 2019, 504–514. https://doi.org/10.1093/jofore/fvz025.

Krause, T.R., Russell, J.M., Zhang, R., Williams, J.W., Jackson, S.T., 2018. Late Quaternary vegetation, climate, and fire history of the Southeast Atlantic Coastal Plain based on a 30,000-yr multi-proxy record from White Pond, South Carolina, USA. Quat. Res. 91, 861–880. https://doi.org/10.1017/qua.2018.95.

Laderman, A.D., 1989. The ecology of Atlantic white cedar wetlands: a community profile. U.S. Fish and Wildlife Serv. Biol. Rep. (Wash. D C) 85 (7.21).

LaMoreaux, H.K., Brook, G.A., Knox, J.A., 2009. Late Pleistocene and Holocene environments of the southeastern United States from the stratigraphy and pollen content of a peat deposit on the Georgia Coastal Plain. Palaeogeogr. Palaeoclimatol. Palaeoecol. 280, 300–312. https://doi.org/10.1016/j.palaeo.2009.06.017.

Levy, G.F., 1991. The vegetation of the Great Dismal Swamp: a review and an overview. Va. J. Sci. 42, 411–417.

Lewis, I.F., Cocke, E.C., 1929. Pollen analysis of Dismal Swamp peat. J. Elisha Mitchell Sci. Soc. 45, 37–58. https://www.jstor.org/stable/24331910.

Lichtler, W.F., Walker, P.N., 1974. Hydrology of the Dismal Swamp Virginia-North Carolina. U.S. Geological Survey Open-file Report 74–39, 50.

Liu, Z., Otto-Bliesner, B.L., He, F., Brady, E.C., Tomas, R., Clark, P.U., Carlson, A.E., Lynch-Stieglitz, J., Curry, W., Brook, E., Erickson, D., Jacob, R., Kutzbach, J., Cheng, J., 2009. Transient Simulation of Last Deglaciation with a New Mechanism for Bolling Allerod Warming. Science 325 (5938), 310–314. http://www.sciencemag.org/cgi/doi/10.1126/science.1171041.

Liu, Z., Otto-Bliesner, B., Clark, P.U., Lynch-Stieglitz, J., Russell, J.M., 2021. SynTRACE-21: Synthesis of Transient Climate Evolution of the last 21,000 years. Past Glob. Changes Mag. 29, 13–15. https://doi.org/10.22498/pages.29.1.13.

Ludwig, R.F., 2018. Variability and Drivers of Forest Communities at the Great Dismal Swamp. M.S. Thesis, Virginia. Polytechnic Institute, Blacksburg, VA, p. 67.

Ludwig, R.F., McLaughlin, D.L., Wurster, F.C., 2021. Red maple dominance and community homogenization in a disturbed forested wetland. Wetl. Ecol. Manag. 29, 599–615.

Manzano, S., Julier, A.C.M., Dirk, C.J., Razafimanantsoa, A.H.I., Samuels, I., Petersen, H., Gell, P., Hoffman, M.T., Gillson, L., 2020. Using the past to manage the future: the role of palaeoecological and long-term data in ecological restoration. Restor. Ecol. 28, 1335–1342. https://doi.org/10.1111/rec.13285.

Marsicek, J.P., Shuman, B., Brewer, S., Foster, D.R., Oswald, W.W., 2013. Moisture and temperature changes associated with the mid-Holocene *Tsuga* decline in the northeastern United States. Quat. Sci. Rev. 80, 129–142. https://doi.org/10.1016/j.quascirev.2013.09.001.

Marsicek, J., Shuman, B.N., Bartlein, P.J., Shafer, S.L., Brewer, S., 2018. Reconciling divergent trends and millennial variations in Holocene temperatures. Nature (Lond.) 554, 92. https://doi.org/10.1038/nature25464.

Mauquoy, D., Hughes, P., van Geel, B., 2010. A protocol for plant macrofossil analysis of peat deposits. Mires Peat 7, 1–5. http://www.mires-and-peat.net/map07/map_07_06.pdf.

McAndrews, J.H., 1988. Human disturbance of North American forests and grasslands: the fossil pollen record. In: Huntley, T., Webb, T. (Eds.), Vegetation History. Springer, pp. 673–697.

McCary, B.C., 1972. A concentration in Virginia of the Perkiomen Broad Spear Point. Q. Bull. Archaeol. Soc. Virginia 26, 145–149.

Mixon, R.B., Berquist Jr., C.R., Newell, W.L., Johnson, G.H., 1989. Geologic Map and Generalized Cross Sections of the Coastal Plain and Adjacent Parts of the Piedmont. U.S. Geological Survey Miscellaneous Investigations Series Map I-2033, Virginia.

Nash, C., 2020. Middle Woodland Research in Virginia: a review of post-1990 studies.). In: Moore, E.A., Means, B.K. (Eds.), The Archaeology of Virginia's First Peoples. The Archeological Society of Virginia, pp. 123–160.

National Oceanic and Atmospheric Administration station at Suffolk, Lake Kilby (station number USC00448192) (data accessed on 10 January, 2022 from https://www.ncdc.noaa.gov/cdo-web/datatools/normals).

Newby, P.E., Shuman, B.N., Donnelly, J.P., Kamauskas, K.B., Marsicek, J., 2014. Centennial-to-millennial hydrologic trends and variability along the North Atlantic Coast, USA, during the Holocene. Geophys. Res. Lett. 41, 4300–4307. https://doi.org/10.1002/2014GL060183.

Oaks Jr., R.Q., 1965. Post-Miocene stratigraphy and morphology, Outer Coastal Plain, southeastern Virginia. In: PhD Dissertation, Yale University, New Haven, Connecticut.

Oaks Jr., R.Q., Coch, N.K., 1963. Pleistocene sea levels, southeastern Virginia. Science 140, 979–983. https://doi.org/10.1126/science.140.3570.979.

Oaks Jr., R.Q., Whitehead, D.R., 1979. Geologic setting and origin of the Dismal Swamp southeastern Virginia and northeastern North Carolina. In: Kirk Jr., P.W. (Ed.), The Great Dismal Swamp. University Press of Virginia, Charlottesville, VA, pp. 1–24.

Overpeck, J.T., Webb, T., Prentice, I.C., 1985. Quantitative interpretation of fossil pollen spectra - dissimilarity coefficients and the method of modern analogs. Quat. Res. 23, 87–108. https://doi.org/10.1016/0033-5894(85)90074-2.

Parham, P.R., Riggs, S.R., Culver, S.J., Mallinson, D.J., Rink, W.J., Burdette, K., 2013. Quaternary coastal lithofacies, sequence development and stratigraphy in a passive margin setting, North Carolina and Virginia, USA. Sedimentology 60, 503–547. https://doi.org/10.1111/j.1365-3091.2012.01349.x.

Pebesma, E.J., 2004. Multivariable geostatistics in S: The gstat package. Comput. Geosci. 30, 683–691. https://doi.org/10.1016/j.cageo.2004.03.012.

Peebles, P.C., Johnson, G.H., Berquist, C.R., 1984. The middle and late Pleistocene

stratigraphy of the Outer Coastal Plain, southeastern Virginia. Va. Miner. 30, 13−22.

Philbrick, C.T., Bogle, A.L., 1981. The pollen morphology of the native New England species of the genus *Acer* (Aceraceae). Rhodora 83, 237−258. https://www.jstor.org/stable/23311008.

Platt, S.G., Brantley, C.G., 1997. Canebrakes: an ecological and historical perspective. Castanea 62, 8−21. https://www.jstor.org/stable/4034098.

R Core Team, 2021. R: A Language and Environment for Statistical Computing [Manual]. R Foundation for Statistical Computing.

Ramsey, K.W., Tomlinson, J.L., Mattheus, C.R., 2022. A radiocarbon chronology of Holocene climate change and sea-level rise at the Delmarva Peninsula, U.S. Mid-Atlantic Coast. Holocene 32, 3−16. https://doi.org/10.1177/09596836211048282.

Rasmussen, S.O., Andersen, K.K., Svensson, A.M., Steffensen, J.P., Vinther, B.M., Clausen, H.B., Siggaard-Andersen, M.-L., Johnsen, S.J., Larsen, L.B., Dahl-Jensen, D., Bigler, M., Rothlisberger, R., Fischer, H., Goto-Azuma, K., Hansson, M.E., Ruth, U., 2006. A new Greenland ice core chronology for the last glacial termination. J. Geophys. Res. 111, D06102. https://doi.org/10.1029/2005JD006079.

Rotzoll, K., Fletcher, C.H., 2013. Assessment of groundwater inundation as a consequence of sea-level rise. Nat. Clim. Change 3 (5), 477−481. https://doi.org/10.1038/NCLIMATE1725.

Roy, L., Peltier, W.R., 2018. Relative sea level in the Western Mediterranean basin: A regional test of the ICE-7G_NA (VM7) model and a constraint on Late Holocene Antarctic deglaciation. Quat. Sci. Rev. 183, 76−87. https://doi.org/10.1016/j.quascirev.2017.12.021.

Saenger, C., Cronin, T., Thunell, R., Vann, C., 2006. Modelling river discharge and precipitation from estuarine salinity in the northern Chesapeake Bay: application to Holocene palaeoclimate. Holocene 16, 467−477. https://doi.org/10.1191/0959683606hl944rp.

Sawada, M., Viau, A.E., Vettoretti, G., Peltier, W.R., Gajewski, K., 2004. Comparison of North-American pollen-based temperature and global lake-status with CCCma AGCM2 output at 6 cal ka BP. Quat. Sci. Rev. 23, 225−244.

Sayers, D.O., 2006. Diasporan exiles in the Great Dismal Swamp, 1630-1860. Transform. Anthropol. 14, 10−20.

Shaler, N.S., 1890. General account of the fresh-water morasses of the United States, with a description of the Dismal Swamp district of Virginia and North Carolina. In: Powell, J.W. (Ed.), Tenth Annual Report of the Director, 1888-1889: Washington, D.C. Government Printing Office, U.S. Geol. Surv., pp. 255−339

Sharitz, R.R., Mitsch, W.J., 1993. Chapter 8. Southern floodplain forests. In: Martin, W.H., Boyce, S.G., Echternacht, A.C. (Eds.), Biodiversity of the Southeastern United States/Lowland Terrestrial Communities. John Wiley & Sons, Inc., pp. 311−371

Shuman, B., Donnelly, J., 2006. The influence of seasonal precipitation and temperature regimes on lake levels in the northeastern United States during the Holocene. Quat. Res. 65, 44−56. https://doi.org/10.1016/j.yqres.2005.09.001.

Shuman, B., Bravo, J., Kaye, J., Lynch, J.A., Newby, P., Webb III, T., 2001. Late Quaternary water-level variations and vegetation history at Crooked Pond, southeastern Massachusetts. Quat. Res. 56, 401−410. https://doi.org/10.1006/qres.2001.2273.

Simpson, B., 1990. The Great Dismal: a Carolinian's Swamp Memoir. Chapel Hill: The University of North Carolina Press, p. 185.

Simpson, G., 2007. Analogue methods in palaeoecology: using the analogue package. J. Stat. Software 22, 1−29.

Sleeter, R., Sleeter, B.M., Williams, B., Hogan, D., Hawbaker, T., Zhu, Z., 2017. A carbon balance model for the Great Dismal Swamp Ecosystem. Carbon Bal. Manag. 12, 1−20. https://doi.org/10.1186/s13021-017-0070-4.

Spencer, J., Jones, K.B., Gamble, D.W., Benedetti, M.M., Taylor, A.K., Lane, C.S., 2017. Late-Quaternary records of vegetation and fire in southeastern North Carolina from Jones Lake and Singletary Lake. Quat. Sci. Rev. 174, 33−53. https://doi.org/10.1016/j.quascirev.2017.09.001.

Spieran, G.K., Wurster, F.C., 2020. Hydrology and water quality of the Great Dismal Swamp, Virginia and North Carolina, and implications for hydrologic-management goals and strategies. U.S. Geol. Surv. Sci. Investigations Rep. 2020−5100, 104. https://doi.org/10.3133/sir20205100.

Stevens, A., Patterson III., W.A., 1998. Millennium-long fire and vegetation histories of pocosins of southeastern Virginia. Virginia Dept. Conserv. Recreat., Division Nat. Herit., Tech. Rep. 98−17.

Stewart, P.C., 1979. Man and the swamp: the historical dimension. In Kirk, P.W., Jr. (ed.), The Great Dismal Swamp, Univ. Press Virginia, Charlottesville, VA, 57-73..

Stockmarr, J., 1971. Tablets with spores used in absolute pollen analysis. Pollen Spores 13, 615−621.

Stuiver, M., Reimer, P.J., Reimer, R.W., 2022. Calib 8.2 [WWW program] at. http://calib.org. (Accessed 10 February 2022).

Swisher, S.E., Peck, J.A., 2020. Vegetation changes associated with the Younger Dryas from the sediments of Silver Lake, Summit County, Ohio, USA. Ohio J. Sci. 120, 30−38. https://doi.org/10.18061/ojs.v120i2.7095.

Telford, R.J., Birks, H.J.B., 2009. Evaluation of transfer functions in spatially structured environments. Quat. Sci. Rev. 28, 1309−1316. https://doi.org/10.1016/j.quascirev.2008.12.020.

Thompson, R.S., Anderson, K.H., Bartlein, P.J., 1999a. Atlas of relations between climatic parameters and distributions of important trees and shrubs in North America − Introduction and conifers. U.S. Geol. Surv. Prof. Paper 1650-A 269.

Thompson, R.S., Anderson, K.H., Bartlein, P.J., 1999b. Atlas of Relationships between Climatic Parameters and Distributions of Important Trees and Shrubs in North

America − Hardwoods. U.S. Geol. Surv. Prof. Paper 1650-B 423.

Thompson, R.S., Anderson, K.H., Bartlein, P.J., 2000. Atlas of relations between climatic parameters and distributions of important trees and shrubs in North America—Additional conifers, hardwoods, and monocots. U.S. Geol. Surv. Prof. 385. Paper 1650-C.

Toomey, M., Cantwell, M., Colman, S., Cronin, T., Donnelly, J., Giosan, L., Heil, C., Korty, R., Marot, M., Willard, D., 2019. The mighty Susquehanna − extreme floods in eastern North America during the past two millennia. Geophys. Res. Lett. 46, 3398−3407. https://doi.org/10.1029/2018GL080890.

Trachsel, M., Telford, R.J., 2016. Technical note: Estimating unbiased transfer-function performances in spatially structured environments. Clim. Past 12, 1215−1223. https://doi.org/10.5194/cp-12-1215-2016.

Traverse, A., 2007. Paleopalynology. Unwin-Hyman, Boston.

Treat, C.C., Jones, M.C., Brosius, L., Grosse, G., Anthony, K.W., Frolking, S., 2021. The role of wetland expansion and successional processes in methane emissions from northern wetlands during the Holocene. Quat. Sci. Rev. 257, 106864. https://doi.org/10.1016/j.quascirev.2021.106864.

Triplett, J., Oltrogge, K.A., Clark, L.G., 2010. Phylogenetic relationships and natural hybridization among the North American woody bamboos (Poaceae: Bambusoideae: *Arundinaria*). Am. J. Bot. 97, 471−492. https://doi.org/10.3732/ajb.0900244.

Trout III., W.E., 2004. The Great Dismal Swamp Atlas. Virginia Canals and Navigations Society, p. 151.

Vega, A.J., Sui, C.H., Lau, K.M., 1998. Interannual to interdecadal variations of the regionalized surface climate of the United States and relationships to generalized flow parameters. Phys. Geogr. 19, 271−291. https://doi.org/10.1080/02723646.1998.10642651.

U.S. Fish and Wildlife Service, 2006. Great Dismal Swamp National Wildlife Refuge and Nansemond National Wildlife Refuge. Final Comprehensive Conservation Plan: U.S. Fish Wildlife Serv, p. 285. https://www.fws.gov/media/great-dismal-swamp-and-nansemond-nwrs-comprehensive-conservation-plan. accessed 23 July 2022.

Vega, A.J., Rohli, R.V., Sui, C.H., 1999. Climatic relationships to Chesapeake Bay salinity during Southern Oscillation extremes. Phys. Geogr. 20, 468−490. https://doi.org/10.1080/02723646.1999.10642691.

Vinther, B.M., Clausen, H.B., Johnsen, S.J., Rasmussen, S.O., Andersen, K.K., Buchardt, S.L., Dahl-Jensen, D., Seierstad, I.K., Siggaard-Andersen, M.-L., Steffensen, J.P., Svensson, A.M., Olsen, J., Heinemeier, 2006. A synchronized dating of three Greenland ice cores throughout the Holocene. J. Geophys. Res. 111, D13102. https://doi.org/10.1029/2005JD006921.

Wanner, H., Solomina, O., Grosjean, M., Ritz, S.P., Jetel, M., 2011. Structure and origin of Holocene cold events. Quat. Sci. Rev. 30, 3109−3123. https://doi.org/10.1016/j.quascirev.2011.07.010.

Watts, W.A., 1970. The full-glacial vegetation of northwestern Georgia. Ecol. 51, 17−33. http://www.jstor.org/stable/1933597.

Watts, W.A., 1979. Late Quaternary vegetation of central Appalachia and the New Jersey coastal plain. Ecol. Monogr. 49, 427−469. https://doi.org/10.2307/1942471.

Wells, B.W., 1942. Ecological problems of the southeastern United States coastal plain. Bot. Rev. 8, 533−561. https://www.jstor.org/stable/4353276.

Whitehead, D.R., 1964. Fossil pine pollen and full-glacial vegetation in southeastern North Carolina. Ecol. 45, 767−776. https://doi.org/10.2307/1934924.

Whitehead, D.R., 1965. Prehistoric maize in southeastern Virginia. Science 150, 881−993. https://www.jstor.org/stable/1717492.

Whitehead, D.R., 1972. Developmental and environmental history of the Dismal Swamp. Ecol. Monogr. 42, 301−315. https://doi.org/10.2307/1942212.

Whitmore, J., Gajewski, K., Sawada, M., Williams, J.W., Shuman, B., Bartlein, P.J., Minckley, T., Viau, A.E., Webb, T., Shafer, S., Anderson, P., Brubaker, L., 2005. Modern pollen data from North America and Greenland for multi-scale paleoenvironmental applications. Quat. Sci. Rev. 24, 1828−1848. https://doi.org/10.1016/j.quascirev.2005.03.005.

Willard, D.A., Cronin, T.M., 2007. Paleoecology and ecosystem restoration: case studies from Chesapeake Bay and the Florida Everglades. Front. Ecol. Environ. 5, 491−498. https://doi.org/10.1890/070015.

Willard, D.A., Cronin, T.M., Verardo, S., 2003. Late-Holocene climate and ecosystem history from Chesapeake Bay sediment cores, USA. Holocene 13, 201−214. https://doi.org/10.1191/0959683603hl607rp.

Willard, D.A., Bernhardt, C.E., Korejwo, D.A., Meyers, S.R., 2005. Impact of millennial-scale Holocene climate variability on eastern North American terrestrial ecosystems: pollen-based climatic reconstruction. Global Planet. Change 47, 17−35. https://doi.org/10.1016/j.gloplacha.2004.11.017.

Willard, D., Bernhardt, C., Brown, R., Landacre, B., Townsend, P., 2011. Development and application of a pollen-based paleohydrologic reconstruction from the Lower Roanoke River basin, North Carolina, USA. Holocene 21, 305−317. https://doi.org/10.1177/0959683610378876.

Williams, J.W., Shuman, B., 2008. Obtaining accurate and precise environmental reconstructions from the modern analog technique and North American surface pollen dataset. Quat. Sci. Rev. 27, 669−687. https://doi.org/10.1016/j.quascirev.2008.01.004.

Williams, J.W., Schuman, B.N., Webb III, T., 2001. Dissimilarity analyses of late-Quaternary vegetation and climate in eastern North America. Ecol. 82, 3346−3362. https://doi.org/10.1890/0012-9658(2001)082[3346:DAOLQV]2.0.CO;2.

Williams, J.W., Shuman, B., Bartlein, P.J., Whitmore, J., Gajewski, K., Sawada, M., Minckley, T., Shafer, S., Viau, A.E., Webb III, T., Anderson, P.M., Brubaker, L.B.,

Whitlock, C., Davis, O.K., 2006. An Atlas of Pollen−Vegetation−Climate Relationships for the United States and Canada. Amer. Assoc. Strat. Palynol. Found., Dallas, TX, p. 293.

Word, C.S., McLauglin, D.L., Strahm, B.D., Stewart, R.D., Varner, J.M., Wurster, F.C., Amestoy, T.J., Link, N.T., 2022. Peatland drainage alters soil structure and water retention properties. Implications for ecosystem function and management. Hydrol. Proc. https://doi.org/10.1002/hyp.14533.

Ziska, L.H., Caulfield, F.A., 2000. Rising CO_2 and pollen production of common ragweed (*Ambrosia artemisiifolia*), a known allergy-inducing species: implications for public health. Austral. J. Plant Physiol. 27, 893−898.